Published in final edited form as:
Mol Microbiol. 2013 October ; 90(1): 54–71. doi:10.1111/mmi.12347.

The DivJ, CbrA and PleC system controls DivK phosphorylation and symbiosis in *Sinorhizobium meliloti*

Francesco Pini[1], **Benjamin Frage**[2], **Lorenzo Ferri**[3], **Nicole J. De Nisco**[4], **Saswat S. Mohapatra**[1], **Lucilla Taddei**[3], **Antonella Fioravanti**[1], **Frederique Dewitte**[1], **Marco Galardini**[3], **Matteo Brilli**[5,§], **Vincent Villeret**[1], **Marco Bazzicalupo**[3], **Alessio Mengoni**[3], **Graham C. Walker**[4], **Anke Becker**[2], and **Emanuele G. Biondi**[1,*]

[1]Interdisciplinary Research Institute USR3078, CNRS-Université Lille Nord de France, 50 avenue de Halley, Villeneuve d'Ascq Cedex, France

[2]LOEWE Center for Synthetic Microbiology and Department of Biology, Philipps-Universität Marburg, Marburg, Germany

[3]Department of Biology, University of Firenze, via Madonna del Piano 6, I-50015 Sesto Fiorentino, Italy

[4]Department of Biology, Massachusetts Institute of Technology, Cambridge, MA 02139, USA

[5]INRIA Grenoble - Rhône-Alpes, Montbonnot and Laboratoire de Biométrie et Biologie Evolutive, CNRS UMR 5558, Université Lyon 1, INRA, Villeurbanne, France

SUMMARY

Sinorhizobium meliloti is a soil bacterium that invades the root nodules it induces on *Medicago sativa*, whereupon it undergoes an alteration of its cell cycle and differentiates into nitrogen-fixing, elongated and polyploid bacteroid with higher membrane permeability. In *Caulobacter crescentus*, a related alphaproteobacterium, the principal cell cycle regulator, CtrA, is inhibited by the phosphorylated response regulator DivK. The phosphorylation of DivK depends on the histidine kinase DivJ, while PleC is the principal phosphatase for DivK. Despite the importance of the DivJ in *C. crescentus*, the mechanistic role of this kinase has never been elucidated in other *Alphaproteobacteria*.

We show here that the histidine kinases DivJ together with CbrA and PleC participate in a complex phosphorylation system of the essential response regulator DivK in *S. meliloti*. In particular, DivJ and CbrA are involved in DivK phosphorylation and in turn CtrA inactivation, thereby controlling correct cell cycle progression and the integrity of the cell envelope. In contrast, the essential PleC presumably acts as a phosphatase of DivK. Interestingly, we found that a DivJ mutant is able to elicit nodules and enter plant cells, but fails to establish an effective symbiosis suggesting that proper envelope and/or low CtrA levels are required for symbiosis.

INTRODUCTION

Caulobacter crescentus and *Sinorhizobium meliloti* belong to the class of *Alphaproteobacteria*, which includes plant endosymbionts (e.g., *Rhizobium*, *Sinorhizobium*, *Mesorhizobium* and *Azorhizobium*), animal pathogens (e.g., *Brucella*, *Rickettsia*) and plant pathogens (e.g., *Agrobacterium*). *Sinorhizobium meliloti*, one of the most intensively studied of these organisms, is able to elicit the formation of nodules on the roots of plants of

*Corresponding author: emanuele.biondi[at]iri.univ-lille1.fr, +33-(0)3-62531719, +33-(0)3-62531701.
§Present address: Fondazione Edmund Mach/CRI, Functional genomics, San Michele all'Adige, Italy.

the genera *Medicago*, *Melilotus* and *Trigonella* (Horvath *et al.*, 1986). *S. meliloti* induces nodule formation, invades plant cells in the interior of the nodule and then undergoes a cellular differentiation process in order to become a nitrogen-fixing bacteroid. In this differentiation, the cells become elongated and polyploid as a result of endo-reduplication of the genome, which suggests that a cell cycle change may be inherent to the differentiation process (Mergaert *et al.*, 2006; Kobayashi *et al.*, 2009; Van de Velde *et al.*, 2010; Wang *et al.*, 2010).

The cell cycle machinery responsible for DNA replication, cell division, and morphogenesis of polar structures is the engine of every organism and has been extensively studied in *C. crescentus* (reviewed by Curtis and Brun, 2010). Many factors are known to regulate cell cycle progression, most of which are members of the family of two-component signal transduction proteins, which is comprised of histidine kinases and their response regulator substrates. Among these, the essential response regulator CtrA is the master regulator and its activity varies as a function of the cell cycle (Quon *et al.*, 1996; Laub *et al.*, 2002).

In *C. crescentus*, CtrA regulates gene expression of key players in the cell cycle and other processes, and it also blocks DNA replication by binding the origin of replication and thus making it inaccessible to the replication initiation factors. The regulon directly controlled by CtrA comprises genes involved in cell division (*ftsZ*, *ftsA*, *ftsQ* and *ftsW*), proteolysis (*clpP)*, DNA methylation (*ccrM)*, flagellar biogenesis (e.g. *flgBC, fliE* and *fliLM*), stalk biogenesis (*tacA*), pili biogenesis (*pilA)*, and chemotaxis (Skerker and Shapiro, 2000; Wortinger *et al.*, 2000; S E Jones *et al.*, 2001; Laub *et al.*, 2002; Biondi, Jeffrey M Skerker, *et al.*, 2006; Collier *et al.*, 2007). The essential role of CtrA has also been demonstrated in other *Alphaproteobacteria*, such as *Brucella* (Bellefontaine *et al.*, 2002) and *S. meliloti* (Barnett *et al.*, 2001), while in several other species, cells can survive without CtrA. In these cases, this protein only controls dispensable functions, such as motility and chemotaxis (e.g. in *Rhodospirillum* and *Magnetospirillum*) (Bird and MacKrell, 2011; Greene *et al.*, 2012).

In *C. crescentus*, CtrA activity peaks at the predivisional stage (Domian *et al.*, 1997), thanks to a combination of transcriptional, proteolytic and phosphorylation control. CtrA is activated through phosphorylation in a cell-cycle dependent fashion; this is accomplished by an essential phosphorelay, comprised of the hybrid histidine kinase CckA and the histidine phosphotransferase ChpT (Biondi, Reisinger, *et al.*, 2006). ChpT can also shuttle the phosphate from CckA to CpdR, a second response regulator that, together with RcdA, is involved in CtrA proteolysis mediated by the ClpP-ClpX protease (Jenal and Fuchs, 1998; Hung and Shapiro, 2002; Ryan *et al.*, 2002; Ryan *et al.*, 2004; McGrath *et al.*, 2006; Iniesta *et al.*, 2006). The phosphorylated response regulator DivK promotes cell cycle progression because it acts at the top of the phosphorelay, interrupting the phosphate flow towards CtrA and thus promoting DNA replication (Hecht *et al.*, 1995; Wu *et al.*, 1998).

Two histidine kinases, DivJ and PleC, are known to interact with DivK. DivJ plays a role in controlling the length and location of the stalk and the cell division plane (Ohta *et al.*, 1992), while a null *Caulobacter pleC* mutant produces almost symmetric cells at division and shows abnormal polar development (Burton *et al.*, 1997). Phosphorylated DivK also acts as an allosteric activator for DivJ and PleC, triggering PleD-dependent production of cyclic-di-GMP, which ultimately modulates CtrA proteolysis in the stalked compartment (Paul *et al.*, 2008; Abel *et al.*, 2011). In *Caulobacter*, DivJ and PleC are the principal kinase and phosphatase of DivK, respectively (Wheeler and Shapiro, 1999). It should be noted that, although DivK has an essential role and its activation by phosphorylation is crucial, the non-essentiality of DivJ and PleC in *C. crescentus* is still inexplicable.

In other *Alphaproteobacteria*, histidine kinases similar to DivJ/PleC have been described, such as CbrA and PleC in *S. meliloti* and PdhS in *B. abortus* (Gibson *et al.*, 2006; Hallez *et al.*, 2007; Gibson *et al.*, 2007; Mignolet *et al.*, 2010; Fields *et al.*, 2012; Sadowski *et al.*, 2013). Although two-hybrid experiments have shown that PdhS binds DivK in *Brucella*, no direct biochemical demonstration have been provided yet for the other species. Recently, CbrA has been connected to the positive control of DivK phosphorylation in *S. meliloti* (Sadowski *et al.*, 2013), as it is positively responsible for the control of DivK localization, which in turn depends on its phosphorylation state. The investigation of the cell cycle's genetic architecture in *Alphaproteobacteria* has been recently explored using bioinformatics, revealing the conservation of the regulatory network of CtrA and DivK in *Caulobacterales* and the *Rhizobiales* (Brilli *et al.*, 2010), although no direct experimental evidence has been provided.

Here we studied the *S. meliloti* phosphorylation system, consisting of several putative kinases, that controls the essential cell cycle factor DivK. We integrated both *in vivo* and *in vitro* approaches to dissect its architecture and understand its function. Our results indicate that the kinases involved in phosphorylation/dephosphorylation of DivK are essential in *S. meliloti*, a major difference with respect to *Caulobacter* despite the similarities concerning their cell cycle networks. In addition to the defects in the cell cycle caused by loss of DivJ, we show that the absence of DivJ strongly affects the ability of *Sinorhizobium meliloti* to function as an efficient symbiont of *M. sativa*, suggesting a link between cell cycle regulators and symbiosis.

RESULTS AND DISCUSSION

DivJ in *S. meliloti* is involved in cell cycle regulation

In *S. meliloti*, the putative DivJ ortholog is a histidine kinase that is anchored to the membrane and has a sensor region that is divergent from that of the *C. crescentus* DivJ. Instead of having several membrane spanning domains, the sensor region of *S. meliloti* DivJ only contains one (Fig. 1A). In order to study its function, we constructed a *S. meliloti* strain carrying the deletion of the gene SMc00059, encoding DivJ (Hallez *et al.*, 2004; Brilli *et al.*, 2010). The Δ*divJ* (BM253) mutant was viable, but it showed a severe reduction of its doubling time (Fig. 1B). We confirmed the deletion by PCR and excluded the possibility that the phenotypes were caused by polar mutations by using the phage ΦM12 (Finan *et al.*, 1984) to transduce the deletion cassette from BM253 into a strain carrying a plasmid-borne $divJ^+$ and showing that the $divJ^+$ plasmid is indeed able to fully complement all the mutant phenotypes (Fig. 1C). Most of the cells of Δ*divJ* were abnormally shaped (long, branched or short morphologies > 60 %, sampling of 100 cells) and in particular we observed a branched phenotype in 10% of the cells (Fig. 1C), which usually suggests cell division and polarity defects. As in *C. crescentus*, *S. meliloti* Δ*divJ* cells were still motile (assayed by soft agar plates and directly observed by light microscopy, Fig. 1D). The slightly smaller halo of the *divJ* mutant in the soft agar could be due to the slower growth of the mutant and/or the branched phenotype of cells, which usually retards the motility. Confirming the functional annotation, the putative *divJ* of *S. meliloti* was able to complement deletion of *divJ* in *C. crescentus*. In particular, the *C. crescentus* Δ*divJ* growth defect was rescued by expressing *S. meliloti divJ*, which resulted in a change from a doubling time in rich medium of 140 ± 10 min. to 102 ± 8 min (derived from three independent growth curves in each strain), the same as the wild type doubling time of ca. 100 ± 5 min. Moreover the overall morphology of this complemented strain (Fig. 2A) closely resembled that of the wild type cells (cell length corresponding to 90% ± 10% of wild type cells), as compared to Δ*divJ* cell (180% ± 20% of wild type, analyzing 100 cells) and stalk length (120% ± 15% of wild type), as compared to Δ*divJ* (240% ± 20% of normal stalks, analyzing 100 stalked cells).

Next we tested the effect of *divJ* overexpression in *S. meliloti* by constructing a strain in which *divJ* was under the control of an IPTG inducible P_{lac} promoter (pSRK derivatives) (Khan *et al.*, 2008) (BM317). Overexpression of *divJ* caused a severe growth defect as implied by the absence of colony forming units in TY medium with IPTG (Fig. 2B). The strain overexpressing DivJ also showed an elongated cell morphology suggesting a negative effect on cell division (Fig. 2C). Finally, we checked alterations of the DNA content by using flow cytometry analysis (Fig. 2D). This investigation revealed that, after 4 h of overexpression of *divJ*, cells with two genome copies accumulated in comparison with wild type, suggesting a block of cell division at the G2 stage. Overexpression of *divJ(H249A)* (EB775), which is mutated in the conserved histidine putatively required for phosphorylation showed no over-expression phenotypes, suggesting that the histidine in position 249 is necessary for DivJ activity (data not shown). *divJ(H249A)* was also unable to complement the deletion phenotype of the *divJ* mutant (data not shown). As we were unable to obtain a good preparation of DivJ antibodies, we cannot exclude the formal possibility that that instability of the DivJ(H249A) mutant protein may be responsible for the absence of an overexpression phenotype, but we consider this to be very unlikely.

The observation that PleC, the phosphatase that dephosphorylates DivK in *C. crescentus*, is essential in *S. meliloti* (Fields *et al.*, 2012) suggests that severity of *divJ* overexpression may be because higher levels of DivK phosphorylation are not well-tolerated in *S. meliloti*. We speculated then that deletion of *pleC* should be similar to overexpression of *divJ*, and that the over-expression of *divJ* is lethal in *S. meliloti* due to the high levels of DivK-P. This explanation requires that DivJ would be able to transfer phosphate groups to DivK.

In order to confirm that DivJ is in fact a histidine kinase (HK) able to phosphorylate DivK, we purified its HK domain, as predicted by SMART database and used it for phosphorylation biochemical assays. After incubating the DivJ HK domain with ATP, we were able to separate the phosphorylated form of DivJ-HK by Phos™-Tag SDS-PAGE electrophoresis. The phosphorylated form of DivJ-HK accumulated over time indicating auto-kinase activity (Fig. 3A). This auto-phosphorylation is dependent on the presence of the histidine residue H249 since mutation of this residue abolished the autokinase activity (Fig. S1). In order to test the ability of DivJ-P to transfer phosphate to DivK, we removed ATP after DivJ-P had accumulated and added purified DivK or DivK(D53A), incubating at different time points. Results in Fig. 3B showed that DivJ can phosphorylate DivK and that the predicted aspartate receiver residue is required for phosphotransfer. These in vitro phosphotransfer experiments indicate that purified DivJ-HK is able to autophosphorylate and transfer the phosphate to DivK, and that both conserved sites of phosphorylation (H249 and D53 respectively) are required.

DivJ represses CtrA phosphorylation and activity in *S. meliloti*

In *C. crescentus*, DivK inhibits CtrA via DivL/CckA (Biondi, Reisinger, *et al.*, 2006; Tsokos *et al.*, 2011) and triggers c-di-GMP production via PleD (Paul *et al.*, 2008; Abel *et al.*, 2011). If DivJ/DivK function to inhibit CtrA phosphorylation in *S. meliloti*, deletion of *divJ* should lead to a more severe/lethal phenotype when CtrA levels are increased. Using an M12 phage lysate of strain BM253 (Δ*divJ* carrying the resistance cassette for tetracycline), we attempted to transduce the *divJ* deletion, into a strain with *ctrA* under an inducible promoter (BM240), creating the strain BM264. Transductants were recovered only without IPTG in the selective medium (Fig. 4A) indicating that a strain carrying a deletion of *divJ* does not tolerate high levels of CtrA. We further analyzed the strain BM264 grown first without IPTG and then switched to a medium supplemented with IPTG; the strain developed a highly branched and elongated phenotype confirming that overproduction of CtrA results in severe cell cycle defect(s) (Fig. 4B).

To investigate this further, we measured the expression levels of the *pilA* promoter in a Δ*divJ* strain in comparison with wild type cells. In *C. crescentus, pilA* expression is directly controlled by CtrA (Skerker and Shapiro, 2000). We measured the expression of *pilA* by fusing a *pilA* promoter to the *lacZ* gene and measuring β-galactosidase activity. Our results (Fig. 5A) demonstrate higher levels in the *divJ* mutant (EB638), suggesting that CtrA is also more active, consistent with the model of DivJ and DivK inhibiting CtrA activity.

We further tested this model by measuring phosphorylation levels of CtrA in different genetic backgrounds. In order to quantify CtrA-P levels *in vivo*, we used the Phos-Tag system in combination with immunoblots with anti-CtrA antibodies (Fig. 5B). To the best of our knowledge, is the first time in the *S. meliloti* field that in vivo measurements of phosphorylation of a protein have been successfully performed. Cell lysates are loaded on SDS-Page electrophoresis gels and, in contrast to measurements using radioactivity, no specific culture medium is required, as Phos-Tag detects unlabeled wild type proteins. We measured levels of CtrA-P (Figure 5C) in three biological replicates of wild type, Δ*divJ* and *cbrA*: : Tn5 cells (this latter case is discussed in the following sections). Consistent with the increased activity of the CtrA-controlled promoter of *pilA*, levels of phosphorylated CtrA were significantly increased in the Δ*divJ* strain compared to wild type.

In summary, the results discussed in this section show that DivJ, which is able to phosphorylate DivK *in vitro*, is also required for down-regulation of CtrA phosphorylation and subsequently its activity as transcriptional activator. However, this raises the question of whether DivJ is the only histidine kinase controlling DivK phosphorylation in *S. meliloti*.

In silico analysis of histidine kinases predicted to interact with DivK in *S. meliloti*

We employed an *in silico* strategy to identify other genes in *S. meliloti* (extended also to genomes of other *Alphaproteobacteria*) that encode for proteins that belong to the family of histidine kinases that controls DivK phosphorylation and dephosphorylation. This family was named *pleC*/*divJ* homolog sensor family (PdhS) as previously suggested (Hallez *et al.*, 2004). In order to predict the kinases interacting with a response regulator, we took advantage of a previous analysis that defined the regions of the histidine kinase that make contact with the response regulator and that are responsible for the specificity of this interaction (Skerker *et al.*, 2008). This approach was integrated with the hypothesis that all *Alphaproteobacterial* DivK and PleC proteins are able to interact with DivK (Brilli *et al.*, 2010). The fragment of the HK responsible for the specific interaction with the response regulator DivK comprises helix 1 and helix 2 of the two-helix bundle that surrounds the histidine residue (Ohta and Newton, 2003; Skerker *et al.*, 2008). Helix 1 of the *C. crescentus* DivJ corresponds to residues 332 to 351 and helix 2 corresponds to 369 to 395. Results of the alignment of DivJs and PleCs are shown in figure S2. From this alignment, in which we used both helices, we derived a probability model describing the variability at each position of the most conserved helix (helix 1) in DivJ and PleC proteins from organisms possessing DivK (Fig. 6A). We scanned for HKs in *Alphaproteobacteria* genomes using a probability matrix that allowed us to assign a score to each of them, while a threshold chosen to include known DivK partners allowed identifying additional putative DivK interactors. Notably, *S. meliloti* CbrA (Gibson *et al.*, 2007) and the *B. abortus* PdhS (Hallez *et al.*, 2007), which have been hypothesized to interact with DivK, were in fact detected with this bioinformatic analysis. The list of accession numbers of PdhS family members is shown in table S1. *S. meliloti* showed five PdhS kinases including CbrA (Gibson *et al.*, 2006), DivJ and PleC (Fields *et al.*, 2012) and two other histidine kinases putatively belonging to the PdhS family that we named PdhSA and PdhSB (Fig. 6B), SMc04212 and SMc01128 respectively.

DivJ and CbrA are *in vivo* kinases of DivK while PleC acts as a phosphatase

Our prediction identified 5 putative histidine kinases able to interact with DivK, but are those proteins really involved in control of DivK phosphorylation? Previous studies showed that CbrA controls DivK localization by controlling the phosphorylation of DivK (Sadowski *et al.*, 2013). Several other altered phenotypes of the *cbrA* null mutant were reported, such as abnormal EPS production and nodulation defects in alfalfa plants (Gibson *et al.*, 2006; Gibson *et al.*, 2007). PleC is essential in *S. meliloti*, influencing the septum localization and interactions with PodJ (Fields *et al.*, 2012), but no evidence of DivK control by PleC has ever been provided. Mutants of PdhSA and PdhSB, previously generated by mini Tn5 mutagenesis (Pobigaylo *et al.*, 2006), were viable and did not show any abnormal growth or cell cycle phenotype (data not shown). Hence these two latter factors were not analyzed further and we focused on the putative interactions of DivJ, PleC and CbrA with DivK *in vivo*.

First we compared the phenotypes of the *cbrA* and the *divJ* mutants. We tested the ability to bind calcofluor (Gibson *et al.*, 2006), revealing that like the *cbrA*: : Tn5 strain (KEG2016), the Δ*divJ* strain is brighter than wild type; in fact, the *divJ* deletion is much brighter than the *cbrA*: : Tn5 strain (Fig. 7A). Since calcofluor is an indicator of alterations in envelope composition we tested the integrity of the cell envelope /resistance to osmotic stresses of Δ*divJ* by assaying the sensitivity of Δ*divJ* to the hydrophobic dye crystal violet in comparison with the *cbrA*: : Tn5 and wild type cells. Both mutant strains were unable to form single colonies in LB supplemented with the crystal violet, while wild type cells could survive, suggesting an alteration of the cell envelope composition (Fig. 7B). This is interesting because permeability of membranes and resistance to oxidative stress are important factors during the infection of legume hosts (Sharypova *et al.*, 2003; Campbell *et al.*, 2003).

In order to gain more information about the functions controlled by DivJ, transcriptome profile analysis of the *divJ* mutant was performed and compared with the transcriptome profile of *cbrA*: : Tn5 (Gibson *et al.*, 2007). We first determined genes differentially expressed in the *divJ* mutant compared to the wild type (Table 1). The analysis revealed genes that had altered expression in the *divJ* mutant compared with wild type cells; log2 ratios of the mutant vs. wild type are shown. A total of 16 genes were lower in the Δ*divJ* cells, including several flagellar genes (*fliE*, *flgG*, *flaA* and *flab*), as well as chemotactic genes (*mcpU*, *mcpZ* and *cheR*) and genes encoding putative manganese transporters (*sitB* and *sitC*). Also four genes encoding conserved hypothetical proteins, a putative transcription factor gene of the family of *merR*, and *gcvT*, possibly involved in catabolism of glycine were down regulated. Eighteen genes were more highly expressed in the Δ*divJ* cells, ten of which code for hypothetical proteins. Among the genes with an assigned function, *feuP* and five FeuP-controlled genes (Smb20838, SMc00198, Smc01557, SMc01586 and *ndvA*), and the *exoN2* and *pilA* genes, the latter encoding a pilin subunit, were upregulated. FeuP has previously been shown to control several genes such as SMc00198, SMc03900 (*ndvA*), SMc01586, SMc01557 that are required for cyclic glucan export and symbiosis (Griffitts *et al.*, 2008).

A selection of genes suggested to be differentially expressed by the transcriptome data were tested in wild type and Δ*divJ* by fusing the *lacZ* reporter gene to the promoter regions of these genes. We measured β-galactosidase activity in these strains and the results confirmed our transcriptome data (Fig. S3).

Since we had discovered that CtrA activity is higher in a Δ*divJ* strain, (Fig. 5), it was interesting to find that several genes upregulated in this mutant are preceded by a putative CtrA binding site (Brilli *et al.*, 2010). This included the *pilA* promoter whose expression

levels are higher in the Δ*divJ* strain. This observation is consistent with the discovery that CtrA is upregulated in the Δ*divJ* mutant, although the presence of the consensus CtrA site does not establish a regulatory role.

The limited number of genes discovered by the transcriptomic analysis could be explained by the hypothesis that the effects of DivJ may be limited to a short portion of the cell cycle, in which case transcriptional differences in the window of DivJ activity will be blurred in a mixed population.

Many of the genes (19 genes out of 34) putatively controlled by DivJ were also found to be influenced by CbrA (Gibson *et al.*, 2007), indicating a common pathway between the two histidine kinases possibly involving DivK. This observation is also consistent with the observation that both DivJ and CbrA appear to be involved in CtrA activity repression (Figure 5). Additionally, *cbrA*: : Tn5 showed significantly higher levels of CtrA-P (Fig. 5C) suggesting that both DivJ and CbrA participate in similar functions.

Since in *C. crescentus* DivK is essential, we investigated whether DivK was also essential in *S. meliloti*. Using a two-step recombination strategy, we first constructed an *S. meliloti* strain in which *divK* coding sequence was replaced by tetracycline resistance cassette, complemented by the *divK* locus including the promoter. We then selected for excision of the integrative plasmid by plating on sucrose medium. We were able to select sucrose resistant colonies only when the complementing plasmid was present, suggesting the essentiality of DivK (data not shown). To gain additional support for the conclusion that DivK is essential in *S. meliloti*, we also attempted to transduce the *divK* deletion into several genetic backgrounds as reported in Table S2. Again, we were only successful in introducing the *divK* deletion when an extra copy of *divK* was present. These data confirm that is *divK* is essential in *S. meliloti*. We confirmed *in vivo* the importance of the putative phosphorylated site of DivK, the aspartate in position 53 (D53), by overexpressing *divK* and *divK(D53A)*. Overexpression of *divK*, but not overexpression of *divK(D53A)* caused cell cycle defects in *S. meliloti* (Fig. S4, Fig. S4B). DivK overexpression produced cells with abnormal morphologies, resembling the morphological phenotype produced by DivJ overexpression (Fig. S4A).

Next we tested the hypothesis that DivJ and CbrA were synergic, by attempting to combine the deletion of *divJ* with the *cbrA*: : Tn5 mutant, using a phage lysate produced by infection of BM253. Although *cbrA*: : Tn5 is sensitive to phage infection (data not shown), allowing transduction, we could not recover any colonies when we attempted to transduce the *divJ* deletion allele, while the same transduction with wild type as recipient yielded hundreds of colonies (Fig. 4A). This result suggests that the combination of the *divJ* and *cbrA* mutations is lethal in *S. meliloti*. However, we were able to create a double conditional mutant Δ*divJ* and *cbrA*: : Tn5 that was able to survive by expressing *divJ* from an inducible promoter (P_{lac}) in the presence of IPTG, while the transduction without IPTG did not yield any colonies, thereby confirming the lethality of the *divJ cbrA* double mutation (EB602).

To determine the *in vivo* activity of each predicted DivK kinase/phosphatase we measured the DivK phosphorylation levels in different backgrounds (Δ*divJ*, *cbrA*: : Tn5, Δ*pleC*+P_{lac}-*pleC*), as described for CtrA, this time using anti-DivK antibodies raised in rabbit. The anti-DivK antibodies were able to detect two bands in Phos-Tag SDS-Page gels, one of which corresponded to the phosphorylated form that disappeared by boiling the sample, which destroys the labile phosphate bond (Fig. 8A) (Barbieri and Stock, 2008).

Phosphorylation of DivK *in vivo* (Fig. 8B), together with previous results, demonstrated that DivJ is a kinase of DivK and also that CbrA is involved in this DivK phosphorylation, as the level of DivK-P dropped by about half in both strains (Fig. 8C). This result is consistent

with analyses showed in the previous sections for DivJ and similar to the conclusion recently published for CbrA (Sadowski *et al.*, 2013). It also suggests that, as the combination of DivJ and CbrA mutations is lethal, phosphorylation of the essential factor DivK is also essential in *S. meliloti* cells.

We also measured *in vivo* phosphorylation of DivK in the *pleC* depletion strain (EB601). Using 100 uM IPTG, the *pleC* depletion strain showed a mild overexpression of PleC, but had DivK phosphorylation levels similar to Δ*divJ*. After 6 hours of *pleC* depletion DivK-P levels were 2 fold higher than wild type, demonstrating that in *S. meliloti* PleC plays an opposite role of DivJ and is involved in maintaining low levels of DivK-P, as observed in *C. crescentus*.

Next we tested whether it was possible to rescue the lethal phenotype of Δ*pleC* by transducing this deletion in *cbrA*: : Tn5 or Δ*divJ* backgrounds (Table S3). We found that it was only possible to transduce the *pleC* deletion into a strain carrying the *cbrA* mutation (EB630). The observation that only CbrA mutation (not DivJ) is able to rescue the lethality of *pleC* deletion is puzzling but it could be explained by introducing other regulatory levels of these kinases besides the simple contribution to the chemical equilibrium of DivK/DivK-P. For example DivJ, CbrA and PleC could be expressed at different times and/or present in different subcellular locations during the cell cycle. This regulation in time and space could suggest that DivJ is never together PleC while the soluble kinase CbrA could be co-localized with PleC therefore influencing DivK/DivK-P levels at the same time/space as PleC. If this were the case, one possible model is that CbrA functions coordinately with PleC in the same time/space, but that DivJ does not.

In order to test the enzymatic capability of PleC and CbrA to phosphorylate DivK *in vitro*, as we did for DivJ, we attempted to purify both HK domains. We cloned the HK domains of both PleC and CbrA and expressed them in *E. coli* cells. PleC was soluble and purified well, as shown in Fig. S5. In contrast, several preparations of CbrA were all insoluble; therefore no *in vitro* experiments were performed with CbrA. In contrast to the DivJ HK, the preparation of PleC HK did not show any autokinase activity both with either ATP and GTP, suggesting that for PleC the sensor part of the protein and/or specific signals are required to activate this kinase *in vitro*. Alternatively, the kinase domain may not be well folded.

Nevertheless, taken together the in vivo results, the genetic experiments, the high degree of homology of PleC-CbrA-DivJ, and the recent results with CbrA (Sadowski *et al.*, 2013) strongly support a direct role of CbrA and PleC in controlling DivK-P levels.

DivJ activity is required for efficient symbiosis

The alteration of the cell cycle that occurs during bacteroid differentiation in the symbiotic process suggests a possible role for cell cycle regulators, a conjecture supported by previous experiments on the cell cycle regulators CbrA (Gibson *et al.*, 2006) and CpdR (Kobayashi *et al.*, 2009). We therefore tested the ability of the *divJ* mutant (BM253) to nodulate and fix nitrogen in *M. sativa* (Fig. 9). Plants inoculated with the Δ*divJ* mutant had similar appearance and dry weight to non-infected plants, suggesting that nitrogen fixation was impaired (Fig. 9A). The Δ*divJ* mutant was able to induce nodule formation but, compared to the nodules elicited by the wild type strain, these were more abundant, smaller, white, and abnormal in shape (Fig. 9B). Therefore we tested if cells lacking DivJ were able to invade the nodule cells. We infected alfalfa plants using GFP-tagged wild type and Δ*divJ* strains (Fig. 9C). Both nodules of wild type and Δ*divJ* showed GFP signal inside the internal part of the nodule tissue, suggesting infection by bacteria. Sections of nodules containing wild type or Δ*divJ* cells were also stained with the bacteria-specific Toluidine blue and observed under

the microscope (Fig. 9D) in order to understand if mutants were able to enter the plant cells and their ability to proliferate inside. It was evident that Δ*divJ* bacteria were able to infect plant cells inside nodule, however starch accumulation was present, which is usually a sign of inefficient symbiosis. Normally, starch accumulates in root cells before the infection and then when symbiosis is established the granules are quickly metabolized (Hirsch *et al.*, 1983). As expected, the Δ*divJ* strain complemented with wild type *divJ* (BM224) gave a normal symbiotic phenotype (data not shown).

This result suggests that Δ*divJ* is not able to infect efficiently alfalfa plants possibly due to high CtrA levels in Δ*divJ* cells; high CtrA levels may be responsible for the severe symbiotic defects, impairing the ability of the cell to grow, differentiate, or survive in plant cells. As showed before, CtrA protein and phosphorylation levels are both high in Δ*divJ*. Similar results involving a strain with putative high levels of CtrA, were also documented for the null mutant of CpdR, a response regulator required for proper CtrA proteolysis in *C. crescentus* (Kobayashi *et al.*, 2009).

In order to test this hypothesis that CtrA levels or activity should be low in bacteria infecting plant cells, we isolated bacteroids from mature nitrogen fixing nodules and measured CtrA protein levels by immunoblot (Figure S6). The same number of bacteroids and wild type cells was loaded in the SDS-Page gel. Our results clearly showed that CtrA in bacteroids, although more protein content was loaded, was absent. This observation may explain why the deletion mutant of *divJ*, the *cbrA*: : Tn5 mutant, and also the null mutant of *cpdR*, which have all high CtrA levels, are compromised in the establishment of an efficient symbiosis.

Conclusions

Our biochemical and genetic investigation of the histidine kinase DivJ, and its relationship with CbrA and PleC, sheds light on the DivK cell cycle regulatory module in *S. meliloti* and unveils an association between cell cycle regulation and symbiosis. We propose here a model (Fig. 10) in *S. meliloti* where DivJ is a kinase of the essential response regulator DivK. CbrA is also involved in DivK phosphorylation, while PleC, as in *C. crescentus*, may act as phosphatase. Although the putative cell cycle regulated activity (regulation in time) of CbrA, DivJ and PleC and their subcellular localization (regulation in space) have not been completely investigated, we can hypothesize that these kinases create a complex sensory module that is able to coordinate the phosphorylation levels of the essential factor DivK in time and space.

As in *C. crescentus* the phosphorylated DivK acts negatively on CtrA, which in turn plays a positive role for the biogenesis of polar structures and cell division. Unlike in *C. crescentus*, both DivK phosphorylation and dephosphorylation are essential in *S. meliloti*. This essentiality is indicated by the lethality of both the *divJ-cbrA* double mutant and the *pleC* deletion mutant and our *in vivo* phosphorylation data. The comparison between *S. meliloti* and *C. crescentus* suggests that the genetic architecture that controls cell cycle regulation in *Alphaproteobacteria*, although similar in all *Alphaproteobacteria*, also exhibits certain differences, possibly due to different levels of redundancy of feedbacks and regulatory connections. This has been recently observed in *Agrobacterium tumefaciens*, in which cell cycle regulation shows specific characteristics despite being generally similar to the other *Alphaproteobacteria* (Kim *et al.*, 2013).

An interesting feature of the cell cycle defects discovered in *S. meliloti* is the high degree of branching that has been observed when levels of phosphorylated DivK are low. This feature, which is absent in *C. crescentus* cell cycle mutants, may be related to the polar asymmetric growth of peptidoglycan observed in *Rhizobiales* (Brown *et al.*, 2012).

The analysis presented here sheds light on the role of DivJ as kinase of DivK, ultimately inhibiting, as in *C. crescentus*, the CtrA activity as cell cycle transcription factor. However, we cannot exclude that some of the phenotypes we observed in the *S. meliloti* Δ*divJ* may be explained by CtrA abnormally acting on the origin of replication, as described in *C. crescentus*, or by a reduction of the phosphorylation levels of PleD, which is involved in key steps of cell development in *C. crescentus*.

Our investigation of the role of the DivK module during symbiosis revealed that bacteroids are deficient of CtrA and strains with putative high CtrA levels, as the Δ*divJ* in this study, Δ*cbrA* (Sadowski *et al.*, 2013) or the CpdR mutant (Kobayashi *et al.*, 2009) are directly impaired in establishing an efficient symbiosis. As mentioned in the introduction, CpdR is a response regulator that is required for CtrA proteolysis in *C. crescentus*. The *S. meliloti cpdR* mutant showed the ability to penetrate into the nodule and infect plant cells, but it failed to differentiate in bacteroids. Previous studies indicated that bacteroids have an interrupted cell cycle, associated with the multiplication of the chromosome number, a block of cell division, inducing enlargement of cell bodies, and the consequent loss of the ability to multiply (Mergaert *et al.*, 2006).

The ability of the Δ*divJ* mutant to infect alfalfa plant cells and enter the cytoplasm of nodule cells suggest that DivJ is not required in early steps of the infection process outside the roots or inside the infection thread. The symbiotic efficiency, however, is impaired since plants infected by the Δ*divJ* mutant are similar in size to non-inoculated ones and the histology of the nodule tissue revealed many starch granules, typical of inefficient nitrogen fixation. Also the low number of bacteria inside plant cells in comparison with plants infected by wild type suggests problems in the inside the infection thread or endocytosis or multiplication inside the plant cell cytoplasm or problems in the differentiation process. Those problems may be related to the growth defects of the *divJ* mutant observed in the free-living state. Also this symbiotic defect of the *divJ* mutant could be associated with the phenotypes correlated to envelope integrity we observed in this work, such as increased envelope material detected by calcofluor staining or increased sensitivity to oxidative stresses (Fig. 7). However, combined with previous studies, our results suggest that mutations in the cell cycle factors that play a negative role on CtrA (CpdR, DivJ, CbrA) result in a symbiotic defect. Since, DivJ and CbrA, are involved in the inhibition of CtrA, it appears that a high level of CtrA may interfere negatively with the symbiotic process leading to the speculation that bacteroid differentiation requires the down-regulation of CtrA. Direct support for this hypothesis is provided by our discovery that that mature bacteroids have no CtrA. Perhaps plants are able to block cell cycle of infectious rhizobia by affecting the master regulator CtrA. Proper regulation of CtrA may be required to respond to plant inhibitory activity. Alternatively, one could speculate that strains with lower CtrA activities may show a higher symbiotic activity that could be exploited to increase symbiosis efficiency.

EXPERIMENTAL PROCEDURES

Bacterial strains, plasmids, cloning and growth conditions

The bacterial strains and plasmids used in this study are described in Table S4. *Escherichia coli* strains were grown in liquid or solid Luria-Bertani (LB) broth (Sigma Aldrich) (Sambrook *et al.*, 1989) at 37°C supplemented with appropriate antibiotics: kanamycin (50 μg/ml in broth and agar), tetracycline (10μg/ml in broth and agar). *S. meliloti* strains were grown in broth or agar TY (Beringer, 1974) supplemented when necessary with kanamycin (200 μg/ml in broth and agar), streptomycin (500 μg/ml in broth and agar), tetracycline (1 μg/ml in liquid broth, 2 μg/ml in agar), nalidixic acid (10 μg/ml in broth and agar) as necessary. For negative selection 10% sucrose was added to agar plates. For calcofluor analyses, LB agar was buffered with 10 mM MES (morpholine-ethane-sulfonic acid), pH

7.5, and calcofluor white MR2 Tinopal UNPA-GX (Sigma Aldrich) was added at a final concentration of 0.02%.

For conjugation experiments, 1×10^9 *S. meliloti* and 0.5×10^9 *E. coli* S17-1 cells (Simon *et al.*, 1983) were used and incubated 24h at 30° C. For creating the deletion of *divJ, divK* and *pleC*, two fragments of about 1000-bp long amplifying the upstream (P1-P2) and downstream (P3-P4) regions respectively of the target genes were amplified by PCR using specific oligonucleotides (Table S5). For *divJ* the deletion cassette was constructed as previously described (Skerker *et al.*, 2005). For *pleC* and *divK*, instead, restriction enzymes sites for directional forced cloning with the tetracycline resistance cassette were used. All plasmids were then sequenced for verification. The first six and last 12 codons of each gene deleted were left intact to protect against disruption of possible regulatory signals for adjacent genes. Two-step recombination of deletion cassettes was conducted as previously described using integrative plasmid pNPTS138 (Skerker *et al.*, 2005). Deletion of genes was verified by PCR using primers pSmc00059_P1tris, pSmc00059_P4tris, pSmc02369_Pext_fw, pSmc02369_Pext_rv and pSmc02369_Pint_fw, pSmc01371_P1ext and pSmc01371_P4ext··

For transduction, phage and bacteria (in LB containing 2.5 mM $CaCl_2$ and 2.5 mM $MgSO_4$) were mixed to give a multiplicity of infection 1/2 (phage/cell). The mixture was incubated at 30°C for 30 min.

For construction of the complementation plasmid, *divJ* and *pleC* and their putative promoter regions were amplified by PCR using the Rm1021 genomic DNA as template and primers named P1 and P4, for *divK* P1 and P6 primers were used (Table S5). Fragments were gel purified and cloned into the low copy vector pMR10 (Roberts *et al.*, 1996). Plasmids obtained were introduced in *S. meliloti* strains by electroporation (Ferri *et al.*, 2010).

The *divJ* gene for overexpression *in vivo* was amplified from genomic DNA of *S. meliloti* Rm1021 by PCR using pSmc00059_P0 and pSmc00059_P6, digested by restriction (NdeI and XhoI) and ligated in pSRKKm (previously restricted with the same enzymes), generating pSRKKm*divJ*, which was transferred to Rm1021 by electroporation. Similarly pSRKGm-*divJ*, pSRKKm*pleC*, pSRKKm*ctrA* and pSRKKm*divJ*(D249A), pSRKKm*divK* and pSRKKm*divk* (D53A) were constructed.

The *divJ* H249A mutant was constructed with the primers pSmc00059_H249A_sense and pSmc00059_H249A_antisense (Table S5) on the plasmid pSRKKm*divJ* using PfuTurbo DNA polymerase (Stratagene) as previously described (Biondi, Reisinger, *et al.*, 2006).

For β-galactosidase assay, plasmids were constructed by directional forced cloning of pRKlac290 (Alley *et al.*, 1991) digested with BamHI and XbaI with fragments (600bp) of the Smc0360 and Smc0949 promoter regions amplified with the primers pSmc0360_prom_XbaI, pSmc0360_prom_BamHI, pSmc0949_prom_XbaI and pSmc0949_prom_BamHI. β-galactosidase assay was performed as previously described (Fioravanti *et al.*, 2013).

For the efficiency-of-plating (EOP) assays showed in figure 7, cultures were grown to exponential phase (OD_{600}, ≈0.5) in LB/MC medium and then diluted to an OD_{600} of 0.1 of LB. Each sample was serially diluted up to 10^{-6} in LB, and spread onto LB agar containing either crystal violet (Sigma) or IPTG (1mM). After 4 to 5 days of growth at 30°C, the number of CFU was determined, with the exception of the *?divJ* and *cbrA*: : Tn*5* mutant, which required an additional 48 h of growth at 30°C for colonies to appear. The average and standard deviation for each strain were derived from two independent cultures.

FACS analysis

Cells were cultured into LB/MC and grown to OD600 ca. 0.1–0.2 with the appropriate antibiotic. Samples were taken and fixed in 70% ethanol overnight. Fixed cells were centrifuged at and resuspended in 1mL of 50mM sodium citrate buffer plus 100 mg/mL RNaseA and then incubated for two hours at 50° C. After the RNaseA treatment 1uL of a 1:6 dilution of Sytox Green dye (Invitrogen) was added to each sample. Each sample was then read using a FACScan flow cytometer and results were plotted using Flojo software.

Transcriptome analysis: microarray-based gene expression profiling

In this study, we applied the Sm14kOLI microarray carrying 50mer to 70 mer oligonucleotide probes directed against coding and intergenic regions of the *S. meliloti* Rm1021 genome (Galibert *et al.*, 2001). Each of the 6208 coding regions predicted by Galibert et al. (2001) were represented by a single oligonucleotide whereas both strands of the intergenic regions were covered by 8080 oligonucleotides. Intergenic oligonucleotides mapped at distances of ~50 to 150 nucleotides to the intergenic regions. The microarray layout and oligonucleotide sequences are available at ArrayExpress accession no. A-MEXP-1760.

Production and processing of microarrays were done as described in (Brune *et al.*, 2006). Four biological replicates of control strain 1021 or experiment strain BM253 were grown in 100 ml TY supplemented with nalidixic acid medium to an OD600 of 0.6. RNA isolation, cDNA synthesis, labeling, hybridization, image acquisition and data analysis were done as described in (Serrania *et al.*, 2008). To identify significant up- or down-regulated genes, EMMA 2.2 microarray data analysis software (Dondrup *et al.*, 2003) was used for LOWESS normalization and t statistics. Genes were classified as differentially expressed if $p \leq 0.05$ and $M \geq 0.5$ or ≤ -0.5. The M value represents the $\log_2$ ratio between both channels. Microarray data were submitted to ArrayExpress (Accession number).

In vitro and in vivo phosphorylation

We use Phos-tag™ Acrylamide (Nard Chemicals, LTD, Japan) in order to separate and visualize in SDS-Page gels the phosphorylated form (on histidine and aspartate residues) of CtrA, DivJ and DivK as previously described (Barbieri and Stock, 2008). Bands corresponding to the phosphorylated forms of CtrA and DivK were empirically recognized by a simple boiling step that affects specifically the stability of phosphate. Due to this instability all samples were lysed and directly loaded on gels unless specifically indicated.

For biochemical assays (Fig. 3), *S. meliloti* DivJ (just the kinase domain), DivJ H249A (the kinase domain), PleC (the kinase domain), DivK and Divk D53A were PCR amplified using specific primers (Table S5) expressed in *E. coli* BL21 and purified as previously described (Fioravanti *et al.*, 2012). The *divK* D53A mutant was prepared from a plasmid containing wild-type *divK* performing a site-directed mutagenesis with the primers Smc01371_D53A_sense and Smc01371_D53A_antisense (Table S5) using PfuTurbo DNA polymerase (Stratagene) as previously described (Biondi, Reisinger, *et al.*, 2006). Several clones were sequence verified to confirm the presence of the mutation.

Phos-tag™ Acrylamide SDS-PAGE gels (29:1 acrylamide:N,N”-methylene-bis-acrylamide) were prepared with 50 μM Phos-tag™ acrylamide and 100 μM $MnCl_2$ for *in vitro* phosphorylation assays (figure 3) or 25 μM Phos-tag™ acrylamide and 50 μM $MnCl_2$ for *in vivo* phosphorylation analysis (Figures 5 and 8). All gels were run at 4°C under constant voltage (100 V).

In vitro phosphorylation assays were performed using HK 10 μM, ATP 1 μM, $MgCl_2$ 5 mM in HKEDG buffer (10 mM HEPES-KOH pH 8.0, 50 mM KCl, 10% glycerol, 0.1 mM EDTA, 2 mM DTT). Incubation was performed RT and removal of ATP was done by filtration 4 times with HKEDG/Mg buffer using Amicon Ultra 0.5 10 KDa (Millipore).

For *in vivo* analysis, strains were grown to mid-log phase, and then 2ml of the cells were pelleted and stored at −80°C. Pellets were resuspended using a lysis buffer with 10 mM Tris-Cl, pH 7.5 and 4% SDS and incubated at RT for 5 min, then the loading dye was added. Samples were stored on ice for a short time (<10 min) prior to loading onto Phos-tag™ acrylamide gels. Gels were fixed for 10 min in transfer buffer (50 mM Tris-Cl, 40 mM glycine, 15% (v/v) ethanol,) with 1 mM EDTA to remove Mn^{2+} from the gel. Gels were washed 3 times in transfer buffer without EDTA to remove the chelated metal. Immunoblots were performed using Western Blot Signal Enhancer (Thermo Pierce) with rabbit anti-CtrA (1:5000) or anti-DivK (1:2500) primary antibodies. Chemiluminescent detection was performed using Super Signal West Pico Chemiluminescent Substrate (Thermo-Pierce). Bands intensities were analyzed using ImageJ (Schneider *et al.*, 2012).

Nodulation assays and GFP Strains construction

To observe infected cells using eGFP-expressing bacteroids, a mutated constitutive *S. meliloti sinR* promoter region was amplified by PCR from the pSRmig (McIntosh *et al.*, 2009) derivative pSRmigPsinR171mutcc (Matthew McIntosh) using primer pairs psinRmut_fwd and psinRmut_rev. The fragment was inserted into KpnI and XbaI sites of the integrating pG18mob derivative pGEE upstream of EGFP, resulting in vector pGECE. The construct was transferred by *E. coli* S17-1-mediated conjugation to *S. meliloti* Rm1021 or BM253 and integrated into the chromosome by homologous recombination.

Medicago sativa seeds (cv. Eugenia seeds, Samen-Frese, Osnabrück) were surface sterilized and germinated as described (Müller *et al.*, 1988). 48h-old seedlings were transferred to square petri plates containing buffered nodulation medium (BNM) agar (Ehrhardt *et al.*, 1992). The seedlings were inoculated with 200ul bacteria culture, which was grown to logarithmic phase in TY medium supplemented with nalidixic acid and washed in BNM medium. Plant growth and nodule development were screened over the duration of four weeks. After 28 days, plant height, plant dry weight and number of nodules per plant were measured. Images of plant plates and nodules were acquired, and microscopy images of nodule thin cuts were taken.

Bacteroids were extracted from alfalfa mature nodules as previously described (Finan *et al.*, 1983).

Microscopy

S. meliloti cells were grown to mid-log phase, fixed in 70% ethanol, washed, and concentrated with saline solution (0.85% NaCl). Samples were deposited on microscope slides coated with 0.1% poly-L-lysine. Differential interference contrast and fluorescence imaging of nodules was done on a Zeiss Observer Z1 inverted microscope using Zeiss Axiovision software. Exponential phase bacteria were immobilized on 1% agarose slides and imaged using an alpha Plan-Apochromat 100x/1.46 OilDIC objective and Zeiss AxiocamMR3 camera. Nodule thin sections (100 μm) were stained with 16 μM FM4-64 membrane stain, and imaged using an EC Plan-Neofluar 5x/0.16 Ph1 objective and AxiocamMR3 camera, or using a Plan-Apochromat 40x/0.95 DICII objective and AxiocamHRc color camera. Images were processed with ImageJ (Schneider *et al.*, 2012).

Supplementary Material

Refer to Web version on PubMed Central for supplementary material.

Acknowledgments

We gratefully acknowledge support from the Ente Cassa di Risparmio di Firenze (Italy), Accademia dei Lincei (Italy) and Fondazione Buzzati-Traverso (Italy). EGB lab was also supported by ANR (ANR_11_SVJ3_003_01, CASTACC), the Region Nord-Pas-de-Calais (France) and the CPER-CIA. AB lab is supported by the LOEWE program of the State of Hesse (Germany). G.C.W. and N.J.D. were supported by NIH grant GM31010. G.C.W. is an American Cancer Society Professor.

REFERENCES

Abel S, Chien P, Wassmann P, Schirmer T, Kaever V, Laub MT, et al. Regulatory cohesion of cell cycle and cell differentiation through interlinked phosphorylation and second messenger networks. Mol Cell. 2011; 43:550–560. [PubMed: 21855795]

Alley MR, Gomes SL, Alexander W, Shapiro L. Genetic analysis of a temporally transcribed chemotaxis gene cluster in Caulobacter crescentus. Genetics. 1991; 129:333–341. [PubMed: 1660425]

Barbieri CM, Stock AM. Universally applicable methods for monitoring response regulator aspartate phosphorylation both in vitro and in vivo using Phos-tag-based reagents. Anal Biochem. 2008; 376:73–82. [PubMed: 18328252]

Barnett MJ, Hung DY, Reisenauer A, Shapiro L, Long SR. A homolog of the CtrA cell cycle regulator is present and essential in Sinorhizobium meliloti. J Bacteriol. 2001; 183:3204–3210. [PubMed: 11325950]

Bellefontaine A-F, Pierreux CE, Mertens P, Vandenhaute J, Letesson J-J, Bolle XDe. Plasticity of a transcriptional regulation network among alpha-proteobacteria is supported by the identification of CtrA targets in Brucella abortus. Mol Microbiol. 2002; 43:945–960. [PubMed: 11929544]

Biondi EG, Reisinger SJ, Skerker Jeffrey M, Arif M, Perchuk BS, Ryan KR, Laub MT. Regulation of the bacterial cell cycle by an integrated genetic circuit. Nature. 2006; 444:899–904. [PubMed: 17136100]

Biondi EG, Skerker Jeffrey M, Arif M, Prasol MS, Perchuk BS, Laub MT. A phosphorelay system controls stalk biogenesis during cell cycle progression in Caulobacter crescentus. Mol Microbiol. 2006; 59:386–401. [PubMed: 16390437]

Bird TH, MacKrell A. A CtrA homolog affects swarming motility and encystment in Rhodospirillum centenum. Arch Microbiol. 2011; 193:451–459. [PubMed: 21243338]

Brilli M, Fondi M, Fani R, Mengoni A, Ferri L, Bazzicalupo M, Biondi EG. The diversity and evolution of cell cycle regulation in alpha-proteobacteria: a comparative genomic analysis. BMC Syst Biol. 2010; 4:52. [PubMed: 20426835]

Brown PJB, Pedro MAde, Kysela DT, Henst CVan der, Kim J, Bolle XDe, et al. Polar growth in the Alphaproteobacterial order Rhizobiales. Proc Natl Acad Sci USA. 2012; 109:1697–1701. [PubMed: 22307633]

Brune I, Becker Anke, Paarmann D, Albersmeier A, Kalinowski J, Pühler Alfred, Tauch A. Under the influence of the active deodorant ingredient 4-hydroxy-3-methoxybenzyl alcohol, the skin bacterium Corynebacterium jeikeium moderately responds with differential gene expression. J Biotechnol. 2006; 127:21–33. [PubMed: 16890319]

Burton GJ, Hecht GB, Newton A. Roles of the histidine protein kinase pleC in Caulobacter crescentus motility and chemotaxis. J Bacteriol. 1997; 179:5849–5853. [PubMed: 9294444]

Campbell GRO, Sharypova LA, Scheidle H, Jones KM, Niehaus K, Becker Anke, Walker Graham C. Striking complexity of lipopolysaccharide defects in a collection of Sinorhizobium meliloti mutants. J Bacteriol. 2003; 185:3853–3862. [PubMed: 12813079]

Collier J, McAdams HH, Shapiro Lucy. A DNA methylation ratchet governs progression through a bacterial cell cycle. Proc Natl Acad Sci USA. 2007; 104:17111–17116. [PubMed: 17942674]

Curtis PD, Brun Yves V. Getting in the loop: regulation of development in Caulobacter crescentus. Microbiol Mol Biol Rev. 2010; 74:13–41. [PubMed: 20197497]

Domian IJ, Quon KC, Shapiro L. Cell type-specific phosphorylation and proteolysis of a transcriptional regulator controls the G1-to-S transition in a bacterial cell cycle. Cell. 1997; 90:415–424. [PubMed: 9267022]

Dondrup M, Goesmann A, Bartels D, Kalinowski J, Krause L, Linke B, et al. EMMA: a platform for consistent storage and efficient analysis of microarray data. J Biotechnol. 2003; 106:135–146. [PubMed: 14651856]

Ehrhardt DW, Atkinson EM, Long SR. Depolarization of alfalfa root hair membrane potential by Rhizobium meliloti Nod factors. Science. 1992; 256:998–1000. [PubMed: 10744524]

Ferri L, Gori A, Biondi EG, Mengoni A, Bazzicalupo M. Plasmid electroporation of Sinorhizobium strains: The role of the restriction gene hsdR in type strain Rm1021. Plasmid. 2010; 63:128–135. [PubMed: 20097223]

Fields AT, Navarrete CS, Zare AZ, Huang Z, Mostafavi M, Lewis JC, et al. The conserved polarity factor podJ1 impacts multiple cell envelope-associated functions in Sinorhizobium meliloti. Mol Microbiol. 2012; 84:892–920. [PubMed: 22553970]

Finan TM, Hartweig E, LeMieux K, Bergman K, Walker GC, Signer ER. General transduction in Rhizobium meliloti. J Bacteriol. 1984; 159:120–124. [PubMed: 6330024]

Finan TM, Wood JM, Jordan DC. Symbiotic properties of C4-dicarboxylic acid transport mutants of Rhizobium leguminosarum. J Bacteriol. 1983; 154:1403–1413. [PubMed: 6853448]

Fioravanti A, Fumeaux C, Mohapatra SS, Bompard C, Brilli M, Frandi A, et al. DNA Binding of the Cell Cycle Transcriptional Regulator GcrA Depends on N6-Adenosine Methylation in Caulobacter crescentus and Other Alphaproteobacteria. PLoS Genet. 2013; 9:e1003541. [PubMed: 23737758]

Galibert F, Finan TM, Long SR, Puhler A, Abola P, Ampe F, et al. The composite genome of the legume symbiont Sinorhizobium meliloti. Science. 2001; 293:668–672. [PubMed: 11474104]

Gibson KE, Barnett Melanie J, Toman CJ, Long Sharon R, Walker Graham C. The symbiosis regulator CbrA modulates a complex regulatory network affecting the flagellar apparatus and cell envelope proteins. J Bacteriol. 2007; 189:3591–3602. [PubMed: 17237174]

Gibson KE, Campbell GR, Lloret J, Walker Graham C. CbrA is a stationary-phase regulator of cell surface physiology and legume symbiosis in Sinorhizobium meliloti. J Bacteriol. 2006; 188:4508–4521. [PubMed: 16740957]

Greene SE, Brilli M, Biondi EG, Komeili A. Analysis of the CtrA pathway in Magnetospirillum reveals an ancestral role in motility in alphaproteobacteria. J Bacteriol. 2012; 194:2973–2986. [PubMed: 22467786]

Griffitts JS, Carlyon RE, Erickson JH, Moulton JL, Barnett Melanie J, Toman CJ, Long Sharon R. A Sinorhizobium meliloti osmosensory two-component system required for cyclic glucan export and symbiosis. Mol Microbiol. 2008; 69:479–490. [PubMed: 18630344]

Hallez R, Bellefontaine A-F, Letesson J-J, Bolle XDe. Morphological and functional asymmetry in alpha-proteobacteria. Trends Microbiol. 2004; 12:361–365. [PubMed: 15276611]

Hallez R, Mignolet J, Mullem VVan, Wery M, Vandenhaute J, Letesson J-J, et al. The asymmetric distribution of the essential histidine kinase PdhS indicates a differentiation event in Brucella abortus. EMBO J. 2007; 26:1444–1455. [PubMed: 17304218]

Hecht GB, Lane T, Ohta N, Sommer JM, Newton A. An essential single domain response regulator required for normal cell division and differentiation in Caulobacter crescentus. EMBO J. 1995; 14:3915–3924. [PubMed: 7664732]

Hirsch AM, Bang M, Ausubel FM. Ultrastructural analysis of ineffective alfalfa nodules formed by nif: : Tn5 mutants of Rhizobium meliloti. J Bacteriol. 1983; 155:367–380. [PubMed: 6575011]

Horvath B, Kondorosi E, John M, Schmidt J, Török I, Györgypal Z, et al. Organization, structure and symbiotic function of Rhizobium meliloti nodulation genes determining host specificity for alfalfa. Cell. 1986; 46:335–343. [PubMed: 3731273]

Hung, Dean Y.; Shapiro, Lucy. A signal transduction protein cues proteolytic events critical to Caulobacter cell cycle progression. Proc Natl Acad Sci USA. 2002; 99:13160–13165. [PubMed: 12237413]

Iniesta AA, McGrath PT, Reisenauer Ann, McAdams HH, Shapiro Lucy. A phospho-signaling pathway controls the localization and activity of a protease complex critical for bacterial cell cycle progression. Proc Natl Acad Sci USA. 2006; 103:10935–10940. [PubMed: 16829582]

Jenal U, Fuchs T. An essential protease involved in bacterial cell-cycle control. EMBO J. 1998; 17:5658–5669. [PubMed: 9755166]

Jones SE, Ferguson NL, Alley MR. New members of the ctrA regulon: the major chemotaxis operon in Caulobacter is CtrA dependent. Microbiology (Reading, Engl). 2001; 147:949–958.

Khan SR, Gaines J, Roop RM, Farrand SK 2nd. Broad-host-range expression vectors with tightly regulated promoters and their use to examine the influence of TraR and TraM expression on Ti plasmid quorum sensing. Appl Environ Microbiol. 2008; 74:5053–5062. [PubMed: 18606801]

Kim J, Heindl JE, Fuqua C. Coordination of Division and Development Influences Complex Multicellular Behavior in Agrobacterium tumefaciens. PLoS ONE. 2013; 8:e56682. [PubMed: 23437210]

Kobayashi H, Nisco NJDe, Chien P, Simmons LA, Walker Graham C. Sinorhizobium meliloti CpdR1 is critical for co-ordinating cell cycle progression and the symbiotic chronic infection. Mol Microbiol. 2009; 73:586–600. [PubMed: 19602145]

Laub MT, Chen SL, Shapiro Lucy, McAdams HH. Genes directly controlled by CtrA, a master regulator of the Caulobacter cell cycle. Proc Natl Acad Sci USA. 2002; 99:4632–4637. [PubMed: 11930012]

Letunic I, Doerks T, Bork P. SMART 7: recent updates to the protein domain annotation resource. Nucleic Acids Res. 2012; 40:D302–305. [PubMed: 22053084]

McGrath PT, Iniesta AA, Ryan KR, Shapiro Lucy, McAdams HH. A dynamically localized protease complex and a polar specificity factor control a cell cycle master regulator. Cell. 2006; 124:535–547. [PubMed: 16469700]

McIntosh M, Meyer S, Becker Anke. Novel Sinorhizobium meliloti quorum sensing positive and negative regulatory feedback mechanisms respond to phosphate availability. Mol Microbiol. 2009; 74:1238–1256. [PubMed: 19889097]

Mergaert P, Uchiumi T, Alunni Benoît, Evanno G, Cheron A, Catrice O, et al. Eukaryotic control on bacterial cell cycle and differentiation in the Rhizobium-legume symbiosis. Proc Natl Acad Sci USA. 2006; 103:5230–5235. [PubMed: 16547129]

Mignolet J, Henst CVan der, Nicolas C, Deghelt M, Dotreppe D, Letesson J-J, Bolle XDe. PdhS, an old-pole-localized histidine kinase, recruits the fumarase FumC in Brucella abortus. J Bacteriol. 2010; 192:3235–3239. [PubMed: 20382762]

Müller P, Hynes M, Kapp D, Niehaus K, Pühler Alfred. Two classes of Rhizobium meliloti infection mutants differ in exopolysaccharide production and in coinoculation properties with nodulation mutants. Mol Gen Genet. 1988; 211:17–26.

Ohta N, Lane T, Ninfa EG, Sommer JM, Newton A. A histidine protein kinase homologue required for regulation of bacterial cell division and differentiation. Proc Natl Acad Sci USA. 1992; 89:10297–10301. [PubMed: 1438215]

Ohta, Noriko; Newton, Austin. The core dimerization domains of histidine kinases contain recognition specificity for the cognate response regulator. J Bacteriol. 2003; 185:4424–4431. [PubMed: 12867451]

Paul R, Jaeger T, Abel S, Wiederkehr I, Folcher M, Biondi EG, et al. Allosteric regulation of histidine kinases by their cognate response regulator determines cell fate. Cell. 2008; 133:452–461. [PubMed: 18455986]

Pobigaylo N, Wetter D, Szymczak S, Schiller U, Kurtz S, Meyer F, et al. Construction of a large signature-tagged mini-Tn5 transposon library and its application to mutagenesis of Sinorhizobium meliloti. Appl Environ Microbiol. 2006; 72:4329–4337. [PubMed: 16751548]

Quon KC, Marczynski GT, Shapiro L. Cell cycle control by an essential bacterial two-component signal transduction protein. Cell. 1996; 84:83–93. [PubMed: 8548829]

Roberts RC, Toochinda C, Avedissian M, Baldini RL, Gomes SL, Shapiro L. Identification of a Caulobacter crescentus operon encoding hrcA, involved in negatively regulating heat-inducible transcription, and the chaperone gene grpE. J Bacteriol. 1996; 178:1829–1841. [PubMed: 8606155]

Ryan KR, Huntwork S, Shapiro Lucy. Recruitment of a cytoplasmic response regulator to the cell pole is linked to its cell cycle-regulated proteolysis. Proc Natl Acad Sci USA. 2004; 101:7415–7420. [PubMed: 15123835]

Ryan KR, Judd EM, Shapiro Lucy. The CtrA response regulator essential for Caulobacter crescentus cell-cycle progression requires a bipartite degradation signal for temporally controlled proteolysis. J Mol Biol. 2002; 324:443–455. [PubMed: 12445780]

Sadowski C, Wilson D, Schallies K, Walker G, Gibson KE. The Sinorhizobium meliloti sensor histidine kinase CbrA contributes to free-living cell cycle regulation. Microbiology (Reading, Engl). 2013

Sambrook, J.; Fritsch, EF.; Maniatis, T. Molecular cloning: a laboratory manual. Cold Spring Harbor Laboratory; 1989.

Schneider CA, Rasband WS, Eliceiri KW. NIH Image to ImageJ: 25 years of image analysis. Nat Methods. 2012; 9:671–675. [PubMed: 22930834]

Serrania J, Vorhölter F-J, Niehaus K, Pühler Alfred, Becker Anke. Identification of Xanthomonas campestris pv. campestris galactose utilization genes from transcriptome data. J Biotechnol. 2008; 135:309–317. [PubMed: 18538881]

Sharypova LA, Niehaus K, Scheidle H, Holst O, Becker Anke. Sinorhizobium meliloti acpXL mutant lacks the C28 hydroxylated fatty acid moiety of lipid A and does not express a slow migrating form of lipopolysaccharide. J Biol Chem. 2003; 278:12946–12954. [PubMed: 12566460]

Simon R, Priefer U, Pühler A. A Broad Host Range Mobilization System for In Vivo Genetic Engineering: Transposon Mutagenesis in Gram Negative Bacteria. Nat Biotech. 1983; 1:784–791.

Skerker JM, Shapiro L. Identification and cell cycle control of a novel pilus system in Caulobacter crescentus. EMBO J. 2000; 19:3223–3234. [PubMed: 10880436]

Skerker, Jeffrey M.; Perchuk, BS.; Siryaporn, A.; Lubin, EA.; Ashenberg, O.; Goulian, M.; Laub, MT. Rewiring the specificity of two-component signal transduction systems. Cell. 2008; 133:1043–1054. [PubMed: 18555780]

Skerker, Jeffrey M.; Prasol, MS.; Perchuk, BS.; Biondi, EG.; Laub, MT. Two-component signal transduction pathways regulating growth and cell cycle progression in a bacterium: a system-level analysis. PLoS Biol. 2005; 3:e334. [PubMed: 16176121]

Tsokos CG, Perchuk BS, Laub MT. A dynamic complex of signaling proteins uses polar localization to regulate cell-fate asymmetry in Caulobacter crescentus. Dev Cell. 2011; 20:329–341. [PubMed: 21397844]

Velde, WVan de; Zehirov, G.; Szatmari, A.; Debreczeny, M.; Ishihara, H.; Kevei, Z., et al. Plant peptides govern terminal differentiation of bacteria in symbiosis. Science. 2010; 327:1122–1126. [PubMed: 20185722]

Wang D, Griffitts J, Starker C, Fedorova E, Limpens E, Ivanov S, et al. A nodule-specific protein secretory pathway required for nitrogen-fixing symbiosis. Science. 2010; 327:1126–1129. [PubMed: 20185723]

Wheeler RT, Shapiro L. Differential localization of two histidine kinases controlling bacterial cell differentiation. Mol Cell. 1999; 4:683–694. [PubMed: 10619016]

Wortinger M, Sackett MJ, Brun YV. CtrA mediates a DNA replication checkpoint that prevents cell division in Caulobacter crescentus. EMBO J. 2000; 19:4503–4512. [PubMed: 10970844]

Wu J, Ohta N, Newton A. An essential, multicomponent signal transduction pathway required for cell cycle regulation in Caulobacter. Proc Natl Acad Sci USA. 1998; 95:1443–1448. [PubMed: 9465034]

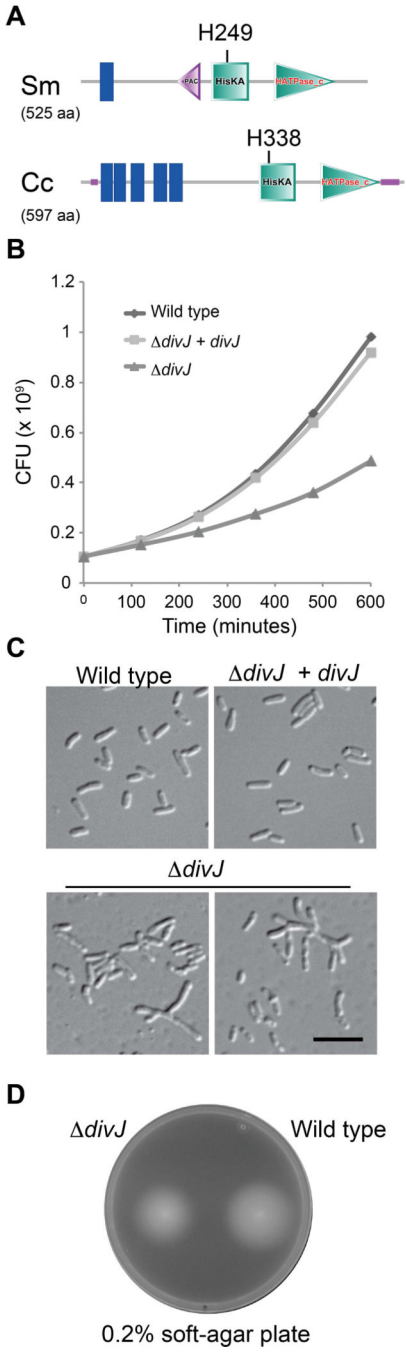

Figure 1. *S. meliloti* Δ*divJ* is viable but shows a cell cycle phenotype

A. Schematics of domain organization of DivJs in *C. crescentus* and *S. meliloti*. Blue bars are the predicted transmembrane regions, the pink triangle is a predicted PAC domain, green squares are the HisKA domains that include the phosphorylated histidine residue, purple horizontal lines are intrinsically disordered regions and finally the HATPase_c domains are the green triangles (analysis performed using SMART database) (Letunic et al., 2102); B. Colony Forming Units (CFU) of wild type, Δ*divJ* (BM253), Δ*divJ*+ *divJ* (BM224). Doubling time (30°C, 180rpm) of BM224 is 200 ± 15 min (similar to wild type cells, 190 ± 13 min), while BM253 doubling time is 284 ± 21 min (standard errors). In figure S7 the same curve is represented in logarithmic scale; C. Cell morphology of the *S. meliloti* wild

type, *divJ* mutant and Δ*divJ*+ *divJ*. Black bar corresponds to 4 μm; D. Soft agar swarmer assay (wild type is 5.6 ± 0.2 cm, while Δ*divJ* is 5.4 ± 0.3 cm after 5 days, standard errors).

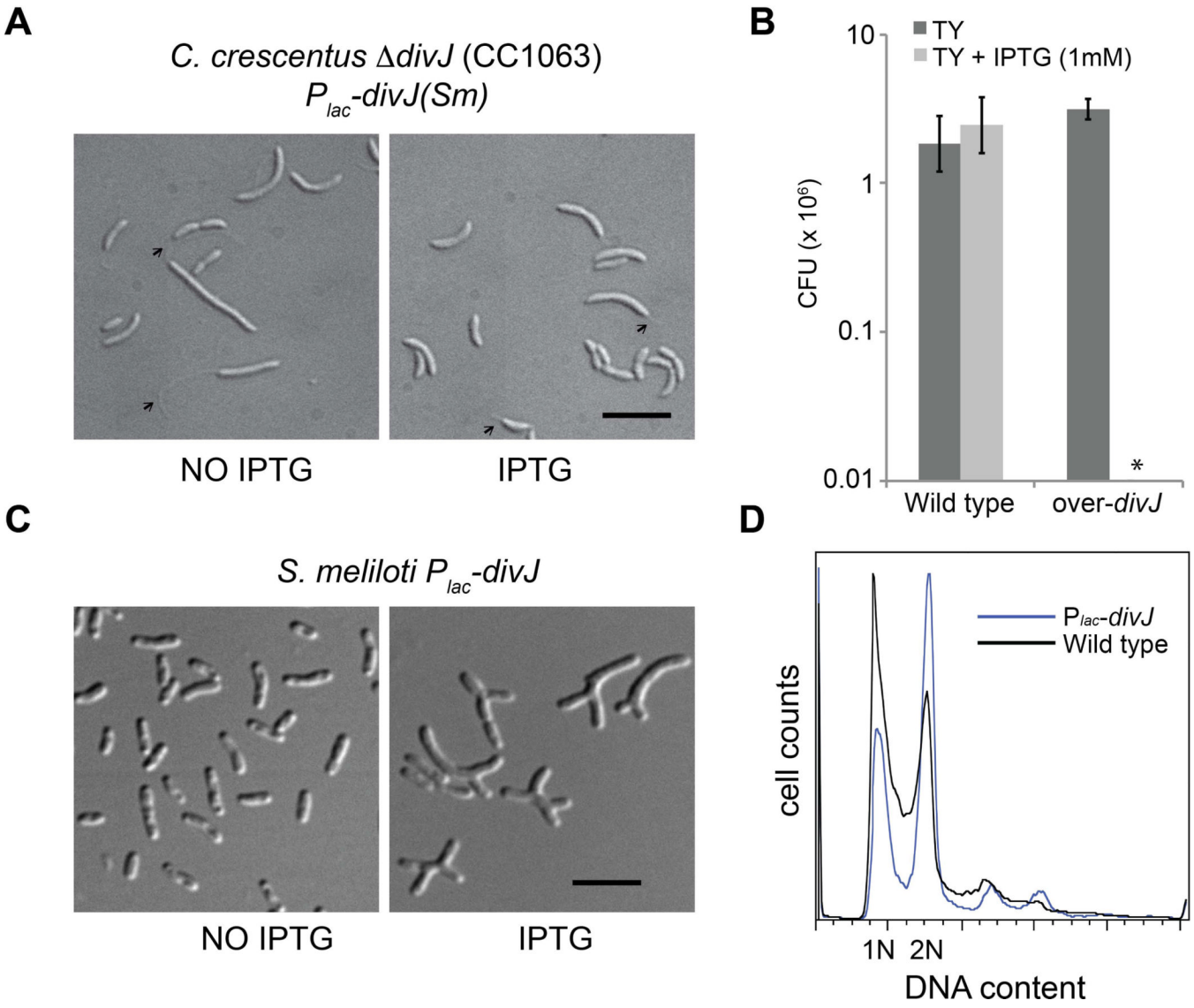

Figure 2. Complementation of *C. crescentus* Δ*divJ* by the *S. meliloti*gene

A. Morphology of *C. crescentus* Δ*divJ* (Skerker *et al.*, 2005) (BM331) and Δ*divJ* complemented (BM333) by an IPTG-inducible copy of *S. meliloti divJ* (100 μM IPTG). Black bar corresponds to 4 μm. Small black arrows indicate stalks. The presence of *S. meliloti divJ* was indeed able to partially rescue the growth defect and the abnormal morphology of *C. crescentus* Δ*divJ* as shown by normal cell morphologies (see text for details). Also the *C. crescentus* Δ*divJ* containing the empty vector (BM331) in IPTG conditions did not show any complementation (Data not shown); B. CFUs of over-*divJ* (BM317) in comparison with wild type cells containing the empty over-expression vector; Cells of cultures grown for 4 hours with or without IPTG, were plated at different dilutions (minimum detectable CFU/ml is 10^4 cells) without IPTG in order to measure the viability (CFU). Clearly the overexpression of *divJ* (IPTG) shows a CFU/ml < 10^4; C. Morphology of over-*divJ*. D. FACS analysis of over-*divJ* in comparison with wild type cells.

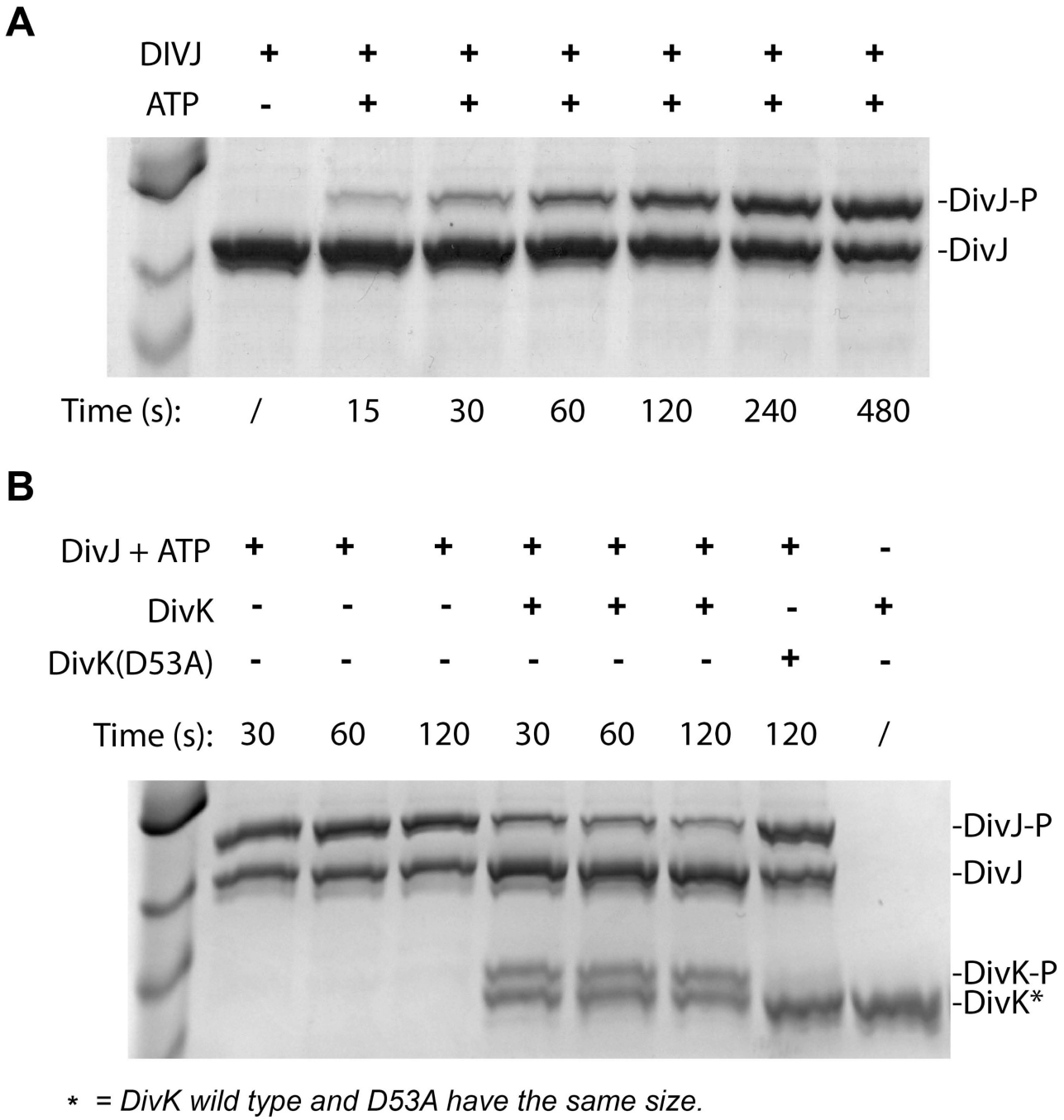

Figure 3. DivJ is a kinase that phosphorylates DivK *in vitro*

A. Purified DivJ histidine kinase domain is able to auto-phosphorylate using ATP as the phosphate source. DivJ in presence of ATP gives two distinct bands in a SDS-PAGE Phos-tag™ gel (Coomassie blue). In particular the amount of phosphorylated band (upper band) increases over time; B. The mutant D53A is not able to receive the phosphate from DivJ.

A

Recipient strain	Number of transduced colonies (CFU/ml)
Wild Type	210
Wild Type IPTG	180
P_{lac} - *ctrA NO IPTG*	230
P_{lac} - *ctrA* IPTG	0
cbrA::Tn5 P_{lac}-*divJ* NO IPTG	0
cbrA::Tn5 P_{lac}-*divJ* IPTG	76

B

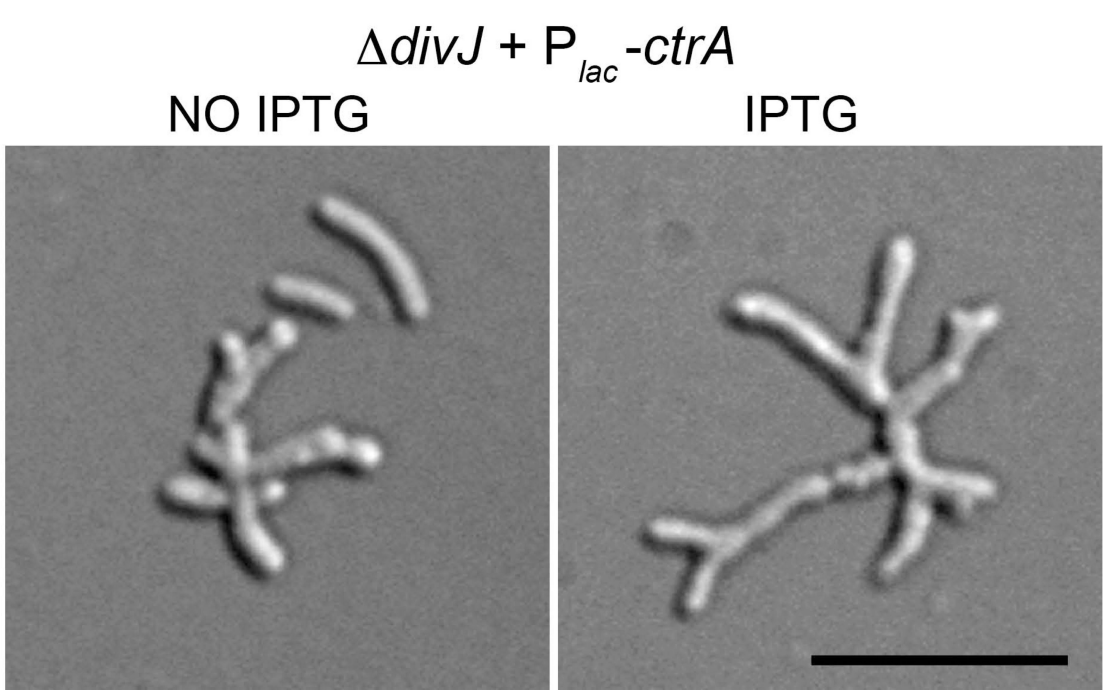

Figure 4. High CtrA levels are lethal in combination with Δ*divJ*

A. Transduction table, in which over-expression of *ctrA* (IPTG) in combination with the Δ*divJ* is lethal; B. Morphology of *S. meliloti* strain BM264 (Δ*divJ* + over-*ctrA*) with and without induction by 1 mM IPTG. The black bar is 3 μm.

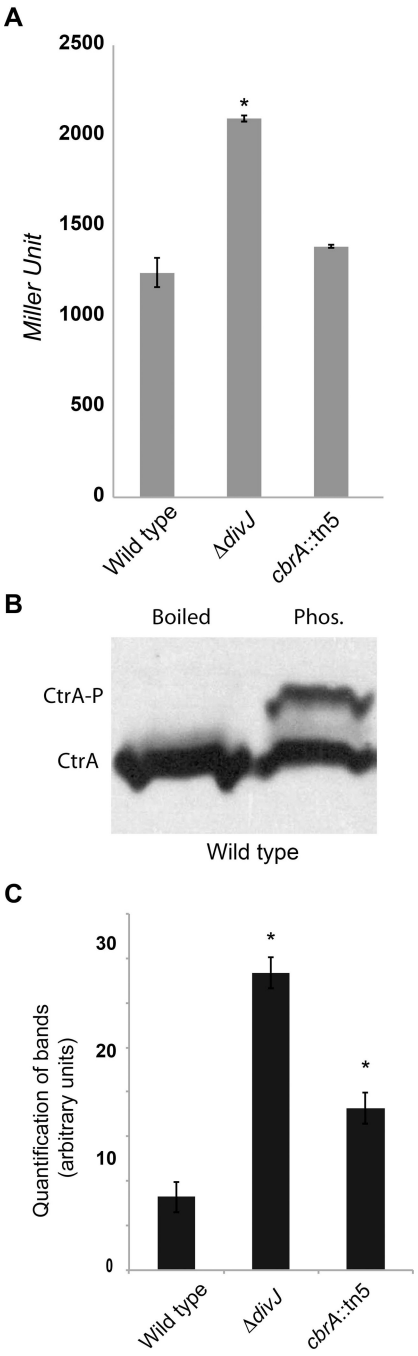

Figure 5. DivJ and CbrA are inhibiting CtrA phosphorylation and activity *in vivo*

A. β-galactosidase activity of a CtrA-controlled promoter in wild type (EB594), Δ*divJ* (EB638) and *cbrA*: : Tn5 (EB593) genetic backgrounds. Experiments were performed in biological triplicates, errors are calculated as standard deviations. Asterisk corresponds to significant statistical difference with wild type conditions (Student's test); B. Phos-tag™ SDS-PAGE gel shows phosphorylation of CtrA *in vivo* in wild type. A lane with SDS-lysed material (Phos.) and another with boiled sample are shown. The phosphorylated band disappears after boiling; C. Quantification of phosphorylation levels of CtrA *in vivo* in wild type, Δ*divJ* and *cbrA*: : Tn5 genetic backgrounds. The average of three experiments using samples at the same OD_{600} is showed, errors are calculated as standard deviations. The

amount of CtrA-P was normalized for the number of cells. Asterisk corresponds to significant statistical difference with wild type conditions (Student's test).

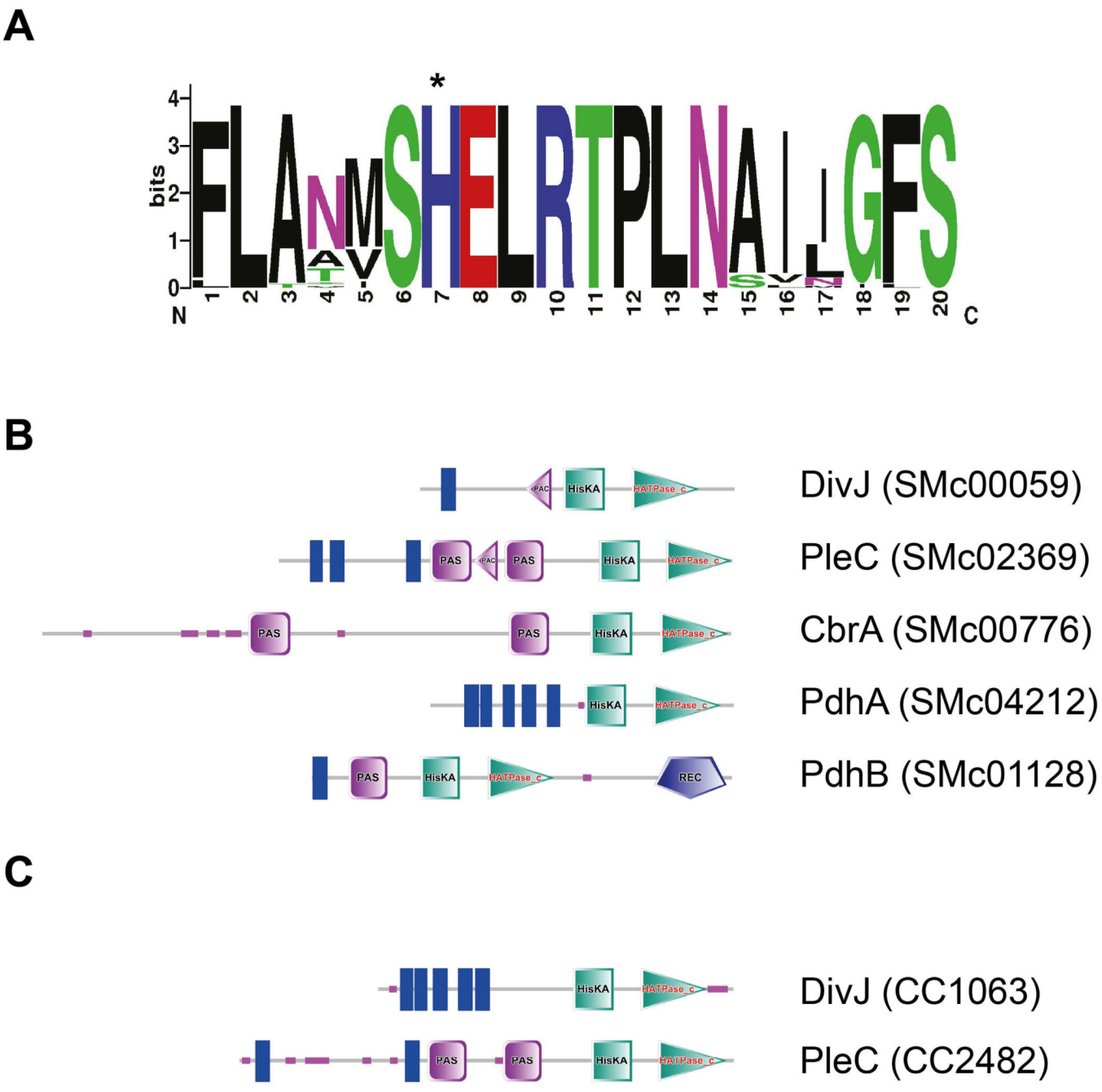

Figure 6. *In silico* analysis of histidine kinases of the PdhS family interacting with DivK

A. PdhS (PleC DivJ Homolog) family specificity consensus based on the alignment in figure S2. Asterisk corresponds to the phosphorylated histidine; B. PdhS-family members in *S. meliloti*; domains were predicted by SMART (Letunic *et al.*, 2012); C. Domains organization of DivJ and PleC in *C. crescentus* predicted by SMART (Letunic *et al.*, 2012). Blue bars are the predicted transmembrane regions, the pink squares are predicted PAS domains, the pink triangles are predicted PAC domains, green squares are the HisKA domains that include the phosphorylated histidine residue, purple horizontal lines are intrinsically disordered regions and finally the HATPase_c domains are the green triangles (analysis performed using SMART database) (Letunic *et al.*, 2012).

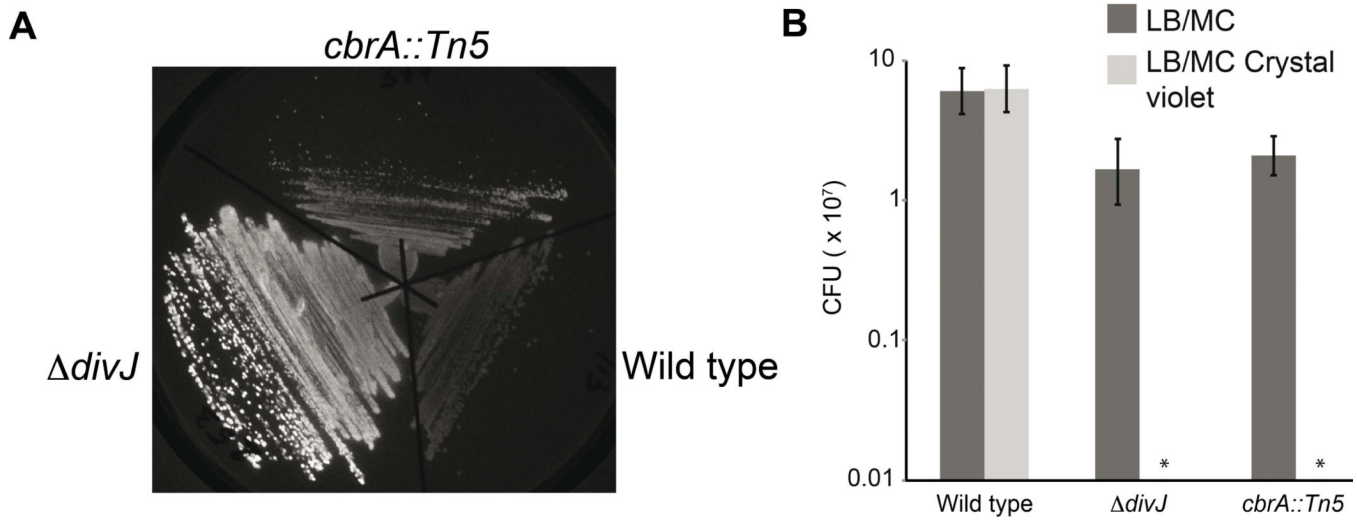

Figure 7. Envelope-related phenotypes of Δ*divJ* and *cbrA*: :Tn5

A. Calcofluor staining of deletion of *divJ* in comparison with wild type and *cbrA*: : Tn5reveals that both *cbrA* and *divJ* mutants are brighter than wild type cells; B. Viable counts of the deletion of *divJ* in comparison with wild type and *cbrA*: : Tn5 with Crystal violet dye revealed that both *divJ* and *cbrA* mutants are sensitive to crystal violet; Cells were plated at different dilutions in LB/MC or LB/MC plus crystal violet in order to measure the viability (CFU) (minimum detectable CFU/ml is 10^5 cells). Clearly Δ*divJ* and *cbrA*: : Tn5 in LB/MC crystal violet show a CFU/ml < 10^5.

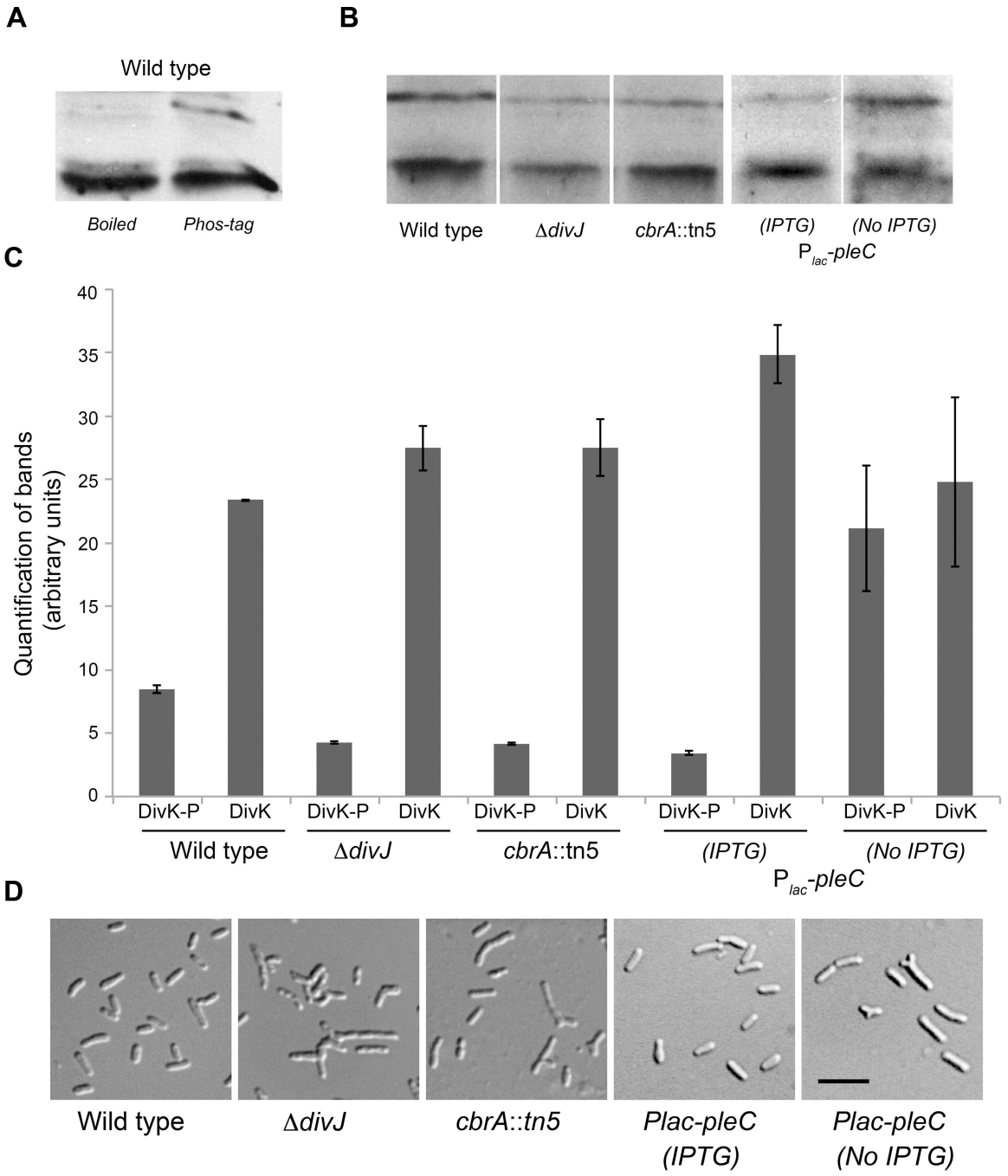

Figure 8. DivJ and CbrA are required for DivK phosphorylation, while PleC acts as a phosphatase

A. SDS-PAGE Phos-tag™ gel detects phosphorylation of DivK *in vivo* in wild type; boiling step ("boiled"), which breaks the phosphate bond, specifically affected the upper band; B. SDS-PAGE Phos-tag™ gel shows phosphorylation of DivK *in vivo* in wild type, Δ*divJ cbrA*: : Tn5 and *pleC* depletion (After 7 h) genetic backgrounds; C. Quantification of phosphorylation levels of DivK *in vivo* in wild type, Δ*divJ cbrA*: : Tn5 and *pleC* depletion genetic backgrounds. The average of three experiments is shown, errors are calculated as standard deviations; D. Morphologies of cells of Δ*divJ cbrA*: : Tn5 and *pleC* depletion

genetic backgrounds. This latter condition is shown with 1mM IPTG and after washes, without IPTG for 7 hours. The black bar corresponds to 3 μm.

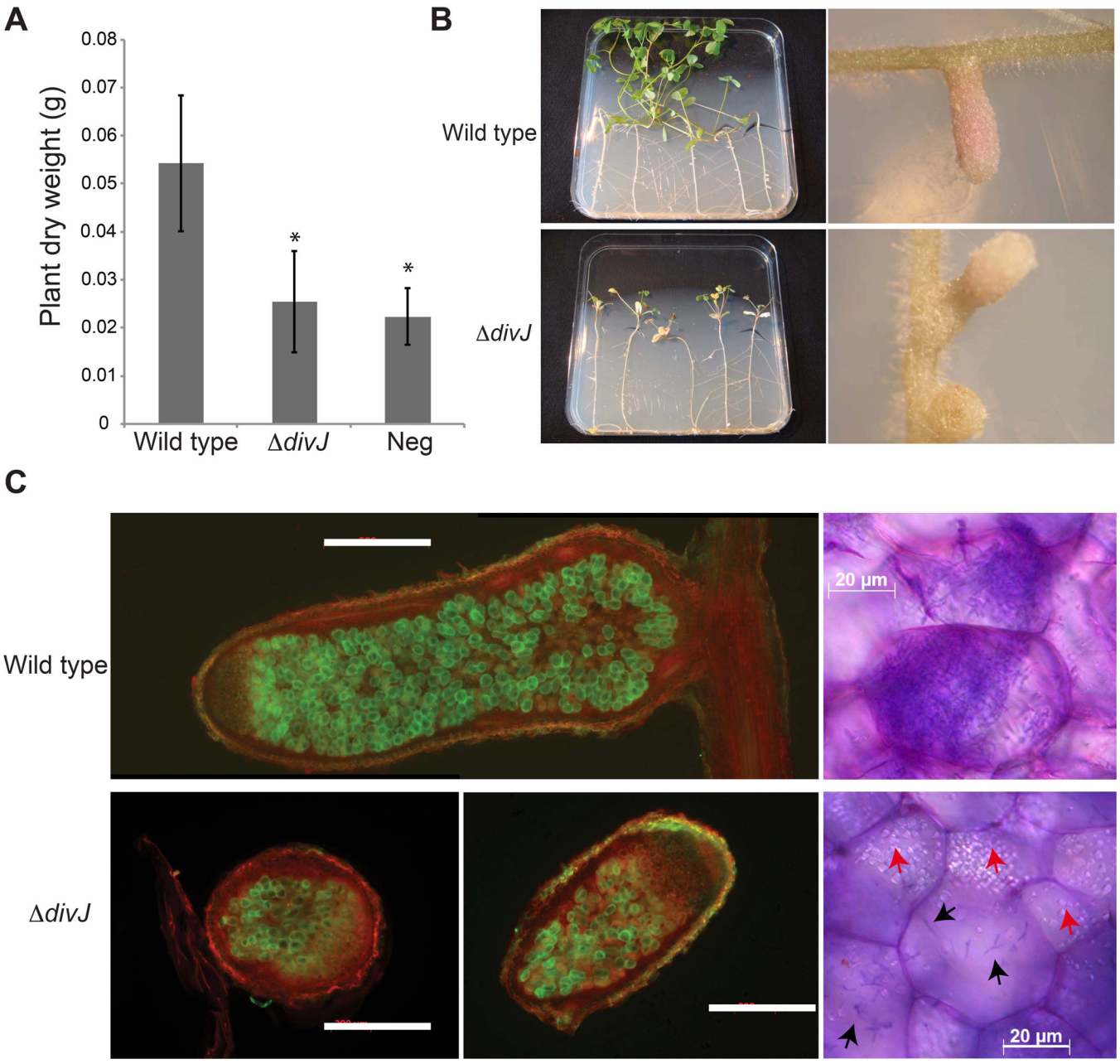

Figure 9. Symbiotic efficiency of Δ*divJ*

A. Histogram with the dry weight of alfalfa plants infected by *S. meliloti* wild type and Δ*divJ* (neg = un-inoculated control). Errors are calculated as standard deviations; B. Pictures of five plants and details on nodules; C. Nodules from an infection of alfalfa plants using GFP-tagged strains (green), wild type is strain Rm1021G and Δ*divJ* is BM253G (Table S4); on the left (white bars correspond to 500 µm) and Toluidine blue staining on the right. Black arrows indicate bacteria inside plants cells, red arrows indicate starch granules.

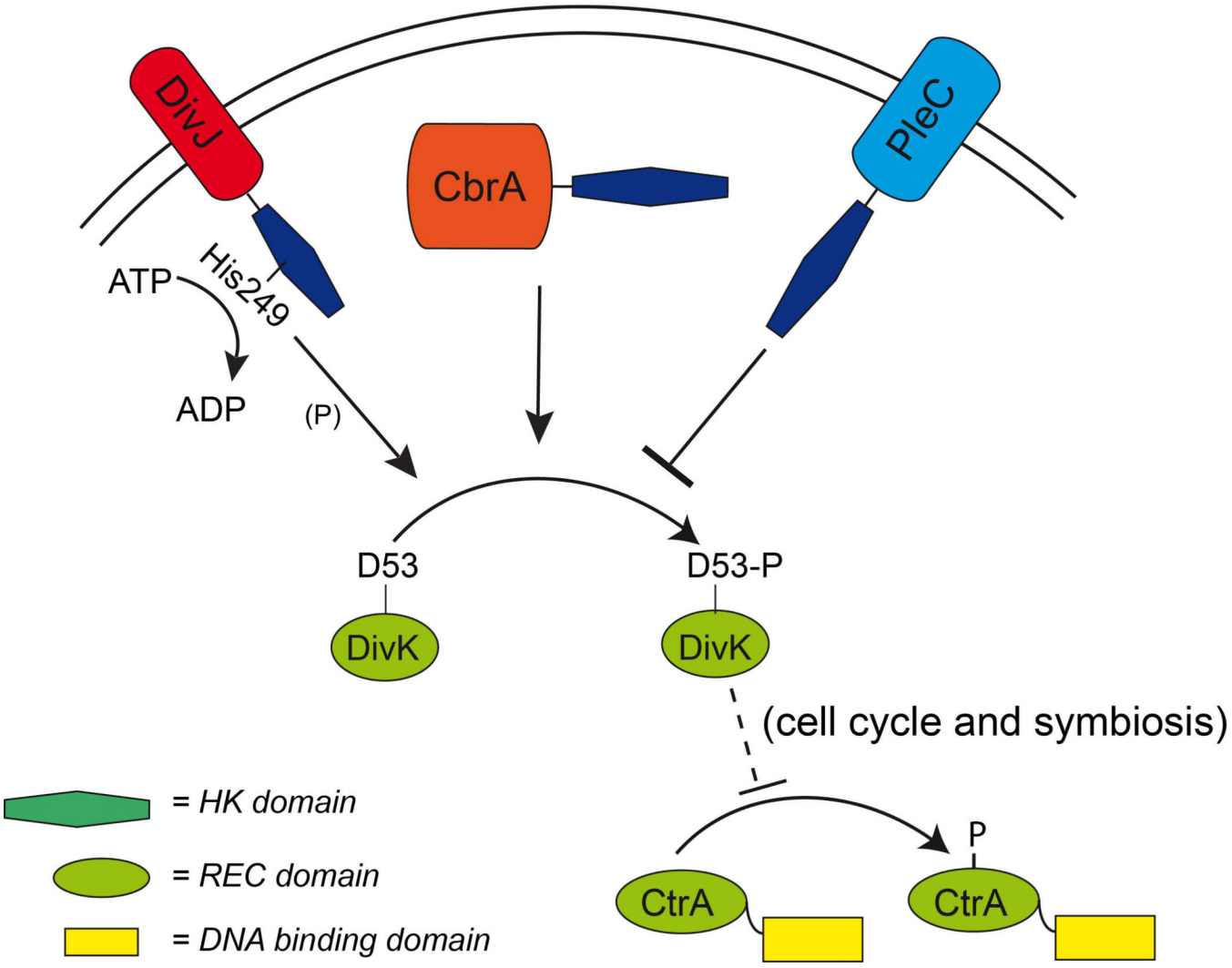

Figure 10. Functional scheme of DivK control system of CtrA

DivK is phosphorylated presumably on the aspartate 53 by the membrane histidine kinase DivJ (using the conserved residue H249 and ATP) and likely by the soluble histidine kinase CbrA. The absence of both kinases from *S. meliloti* is a lethal condition, abolishing DivK phosphorylation. Also the deletion of the membrane histidine kinase PleC is lethal (Fields *et al.*, 2012); results presented here show that PleC is involved in dephosphorylation of DivK. Finally we showed here that DivJ is negatively acting on CtrA and apparently CtrA inactivation is required for an efficient symbiosis, presumably through degradation of the protein. In fact, mature bacteroids do not show detectable CtrA levels, suggesting that one of the symbiotic problems of Δ*divJ* may be the high level of activity of CtrA.

Table 1

Transcriptome profile of the *S. meliloti divJ* deletion with log ratios in comparison with wild type (see Experimental Procedures)

Gene code (Rm1021)	Annotation	Log2-Ratio	CbrA array*	CtrA bs$
Genes with expression reduced in ΔdivJ				
SMa0281	Putative regulator, MerR family	−0.61		
SMc00888	Response regulator	−0.99	y (−)	y
SMc00765	*mcpZ*	−0.65	y (−)	
SMc00975	*mcpU*	−0.52	y (−)	
SMc03009	*cheR*	−0.63	y (−)	
SMc02047	*gcvT*	−0.51		
SMc02507	*sitC*	−0.54		
SMc02508	*sitB*	−0.64		
SMc03029	*fliE*	−0.58	y (−)	
SMc03030	*flgG*	−0.72	y (−)	
SMc03037	*flaA*	−0.51	y (−)	y
SMc03038	*flaB*	−0.78	y (−)	
SMc02104	Conserved hypothetical protein	−0.57		
SMc00360	Conserved hypothetical protein	−0.62	y (−)	y
SMc03013	Conserved hypothetical protein	−0.66	y (−)	
SMc03057	Conserved hypothetical protein	−0.51	y (−)	
Genes with expression increased in ΔdivJ				
SMb20838	putative secreted calcium-binding protein	0.57	y (+)	
SMc00949	Conserved hypothetical protein	0.76	y (+)	
SMc01557	Hypothetical signal peptide protein	0.74	y (+)	
SMa1043	Hypothetical protein	1.45		
SMb21069	Hypothetical protein	2.16		
SMb21440	Hypothetical protein	1.16	y (+)	
SMc00198	Hypothetical protein	0.59	y (+)	
SMc01586	Hypothetical protein	0.75	y (+)	
SMc03999	Hypothetical protein	0.65		
SMc02051	Conserved hypothetical protein	0.56		y
SMc02052	Conserved hypothetical protein	0.56		
SMc02266	Conserved hypothetical protein	0.83	y (+)	
SMc02900	Conserved hypothetical protein	0.96		
SMc03100	Conserved hypothetical protein	0.66		
SMc00458	*feuP*	1.48		
SMc03900	*ndvA*	0.54	y (+)	
SMc04023	*exoN2*	0.55		

Gene code (Rm1021)	Annotation	Log2-Ratio	CbrA array*	CtrA bs$
Genes with expression reduced in ΔdivJ				
SMc04114	*pilA1*	0.54		y

*y(−) means that the same gene was downregulated in the *cbrA* mutant arrays (Gibson *et al.*, 2007); y(+) means that the gene was upregulated also in the *cbrA* arrays.

$= bs., binding site, the prediction is based on Brilli et al., 2010.